

Article

# A Robust Flexible Optimization Model for 3D-Layout of Interior Equipment in a Multi-Floor Satellite

Masoud Hekmatfar <sup>1,2</sup>, M. R. M. Aliha <sup>1,\*</sup> , Mir Saman Pishvaeae <sup>2</sup> and Tomasz Sadowski <sup>3,\*</sup> 

<sup>1</sup> Welding and Joining Research Center, School of Industrial Engineering, Iran University of Science and Technology (IUST), Narmak 16846-13114, Iran; m\_hekmatfar97@ind.iust.ac.ir

<sup>2</sup> School of Industrial Engineering, Iran University of Science and Technology (IUST), Narmak 16846-13114, Iran; pishvaeae@iust.ac.ir

<sup>3</sup> Department of Solid Mechanics, Lublin University of Technology, Nadbystrzycka 40 Str., 20-618 Lublin, Poland

\* Correspondence: mrm\_aliha@iust.ac.ir (M.R.M.A.); t.sadowski@pollub.pl (T.S.)

**Abstract:** Defanging equipment layout in multi-floor satellites consists of two primary tasks: (i) allocating the equipment to the satellite's layers and (ii) placing the equipment in each layer individually. In reviewing the previous literature in this field, firstly, the issue of assigning equipment to layers is observed in a few articles, and regarding the layout, the non-overlapping constraint has always been a challenge, particularly for components that do not have a circular cross-section. In addition to presenting a heuristic method for allocating equipment to different layers of the satellite, this article presents a robust flexible programming model (RFPM) for the placement of equipment at different layers, taking into account the inherent flexibility of the equipment in terms of placement and the subject of uncertainty. This model is based on the existing uncertainty between the distances between pieces of cuboid equipment, which has not been addressed in any of the previous research, and by comparing its outputs with cases from past studies, we demonstrate a significantly higher efficiency related to placing the equipment and meeting the limit of non-overlapping constraints between the equipment. Finally, it would be possible to reduce the design time in the conceptual and preparatory stages, as well as the satellite's overall size, while still satisfying other constraints such as stability and thermal limitations, moments of inertia and center of gravity.



**Citation:** Hekmatfar, M.; Aliha, M.R.M.; Pishvaeae, M.S.; Sadowski, T. A Robust Flexible Optimization Model for 3D-Layout of Interior Equipment in a Multi-Floor Satellite. *Mathematics* **2023**, *11*, 4932. <https://doi.org/10.3390/math11244932>

Academic Editor: Matjaz Skrinar

Received: 28 October 2023

Revised: 5 December 2023

Accepted: 7 December 2023

Published: 12 December 2023



**Copyright:** © 2023 by the authors. Licensee MDPI, Basel, Switzerland. This article is an open access article distributed under the terms and conditions of the Creative Commons Attribution (CC BY) license (<https://creativecommons.org/licenses/by/4.0/>).

**Keywords:** satellite components/equipment 3D layout; uncertainty; proposed robust flexible programming model (RFPM); optimization algorithm

**MSC:** 90C17

## 1. Introduction

In the system design phase of a satellite, layout design is the key step that determines whether the aggregation of functional components from different subsystems can operate normally and smoothly in the space environment throughout its design lifespan or not.

The main aim of satellite layout design is to place the objects or equipment (called components) in the proper positions and orientations to meet various engineering requirements or constraints [1].

As the problem of component layout in a satellite occurs in a limited 3D space, the study of three-dimensional layout would help us to investigate and find the best choices for satellite components' layout. Another important criterion in satellite component layout is the multi-floor concept, due to the space of the satellite containing different layers. Ahmadi, A., et al. [2] undertook a comprehensive survey of multi-floor layouts, and provided a complete overview of the models and solution methods applied for multi-floor facility layout problems.

One of the practical problems with satellite layout is related to the measurement of the distance between pieces of equipment under uncertainty. This type of planning is related to epistemic uncertainty, in which either the data are incomplete or the essence of the problem has an imprecise definition. Here, the opinion of the decision-maker (DM) is not considered, and the uncertainty is related to the data of the problem. On the other hand, flexible programming is used when the constraints are soft and flexibility is considered for the final value of the objective function. Here, the DM has the flexibility required to satisfy the constraints or the value of the objective function, and even though the data are certain, the DM can comment on the uncertainty of the information.

The uncertainty concept plays a significant role in determining the distances between cuboid equipment to solve the overlapping issue in satellite layout by applying flexible programming in determining the distances between pieces of equipment, which is the major contribution of this article.

The rest of this article is structured as follows: A thorough analysis of earlier investigations is provided in Section 1.1. The multi-layer satellite equipment layout problem and related mathematical model are presented in Section 1.2. The problem statement and solution of the integration optimization problem are presented in Section 2, which includes two steps of equipment allocation to bearing layers and then a thorough description of the layout of each layer.

The findings of the sensitivity analysis applied to case studies are presented in Section 3, along with a discussion. Finally, Section 4 presents the conclusions.

### 1.1. Literature Review

The works of [3,4] probably contain the first uses of numerical optimization methods in the layout of spacecraft equipment during the conceptual phase. Rocco, E.M., et al. [5] also presented a multi-objective optimization method for a set of satellites to minimize time-limited fuel consumption. A detailed study of approaches and solution algorithms for the arrangement of three-dimensional equipment was presented by [6]. They showed that the use of CAD software for designing the arrangement of equipment, especially in the arrangement of electrical board parts, is very common, while the three-dimensional arrangement of this software is not very efficient and innovative, and meta-innovative methods such as genetic algorithm and simulated annealing (SA) (such as in the research of [7], who used the SA algorithm to investigate the location of three-dimensional equipment with unknown geometric shapes) have been used more widely in this field.

Articles published in the field of satellite layout are summarized in Table 1. In this table, the methods for allocating equipment to the carrier plates or locating the equipment on each plate are specified, and the details of the problems mentioned by the articles as case studies or numerical examples can be observed in this table. As demonstrated in the table, there are only four articles discussing the allocation of equipment between carrier plates, and the rest only considered the DM's opinion or used arrangements from previous articles.

In addition, regarding the dimensions of problem-solving, as illustrated in Table 1, only 11 articles examined issues related to the design of four carrier plates. Three papers by [8–10] adapted the data from [1] to a multi-cabin satellite with 120 components and eight layers, as opposed to the single-cabin satellite of the original article. These three articles, which established the concept of docking two satellites, are excluded from Table 1. In the remaining cases, the layout of the equipment is either described for a smaller number of plates or is limited to the satellite's cabin, with the latter being more suitable for cube-shaped satellites. In the following, most of the research that has been published in the field of satellite equipment arrangement will be introduced.

**Table 1.** Solution methods and dimensions of case studies on satellite component layout in previous articles.

No	References	Allocation Phase	Solving Method for Non-Overlap Constraints	Solving Method for Other Mechanical Constraints (Moment of Inertia, Center of Gravity, ...)	Problem Dimensions			
					Ex. 1		Ex. 2	
					Layers–Components	Component Shapes	Layers–Components	Component Shapes
1	[11]	equally allocated	analytic geometrical and heuristics methods	dynamical equilibrium constraints	2–26	Cuboid and Cylinder		
2	[12]	centripetal balancing method	GA to reach feasible solution near optimality, plus ACO to adjust the situation of each component	centripetal balancing method	4–53	Cuboid and Cylinder		
3	[13]	predetermined	Heuristic artificial individuals adding rules to the initial population of GA	human-guided GA	4–51	Cuboid and Cylinder		
4	[14]	equally allocated	differential evolution (DE) and local search for cylindrical components	combined GA and PSO	2–14	Cylinder		
5	[15]	predetermined	Human–Algorithm knowledge based on the support of GA		4–51	Cuboid and Cylinder		
6	[1]	Hopfield neural network (HNN)	Geometrical Analysis of Compaction and separation algorithms for nonconvex polygons	hybrid GA and PSO	4–32	Cuboid and Cylinder	4–60	Cuboid and Cylinder
7	[16]	predetermined	hybrid knowledge-based method on the basis of human–computer cooperative GA		4–53	Cuboid and Cylinder		
8	[17]	predetermined	heuristic algorithm of oriented bounding box trees	cooperative co-evolutionary scatter search	1–9	Cylinder	4–60	Cuboid and Cylinder
9	[18]	predetermined	Human–Computer Cooperative Coevolutionary Genetic Algorithm (HCCGA)		3–45	Cuboid and Cylinder		

Table 1. Cont.

No	References	Allocation Phase	Solving Method for Non-Overlap Constraints	Solving Method for Other Mechanical Constraints (Moment of Inertia, Center of Gravity, ...)	Problem Dimensions			
					Ex. 1		Ex. 2	
					Layers–Components	Component Shapes	Layers–Components	Component Shapes
10	[19]	-	Analytic Geometrical Method for two circular or two rectangular components	ACO	1–40	Rectangle		
11	[20]	predetermined	Dual-System Variable-Grain Cooperative Coevolutionary Genetic Algorithm (DVGCCGA) to avoid “premature convergence” problem		4–60	Cuboid and Cylinder	2–18	Cylinder
12	[21]	-		two quasi-physical optimization methods for solving the circle packing problem	1–50	Circle		
13	[22]	-		VBA in Excel and SOLIDWORKS	Satellite Cabin-8	Cuboid		
14	[23]	-	MATLAB, NSGA and SOLIDWORKS	a multi-objective methodology by CAD	Satellite Cabin-27	Cuboid and Cylinder		
15	[24]	predetermined	Finite Circle Method (FCM)	simulated annealing (SA) optimization and quasi-Newton method	2–18	Cylinder	3–17	Cuboid and Cylinder
16	[25]	predetermined	projection and no-fit polygon methods	local search and heuristics	4–51	Cuboid and Cylinder	4–53	Cuboid and Cylinder
17	[26]	-		NSGA and SOLIDWORKS	Satellite Cabin-15	Cuboid and Cylinder		
18	[27]	Genetic Algorithm (GA)	heuristic positioning rule	a combined method of ACO and PSO	4–60	Cuboid and Cylinder		
19	[28]	predetermined		Hybrid GA and gradient-based Sequential Quadratic Programming (SQP) considering natural frequency and attitude control constraints	4–53	Cuboid and Cylinder		

Table 1. Cont.

No	References	Allocation Phase	Solving Method for Non-Overlap Constraints	Solving Method for Other Mechanical Constraints (Moment of Inertia, Center of Gravity, ...)	Problem Dimensions			
					Ex. 1		Ex. 2	
					Layers–Components	Component Shapes	Layers–Components	Component Shapes
20	[29]	-	Hybrid GA and gradient-based Sequential Quadratic Programming (SQP) for cylindrical and spherical shapes		1–9	Cylinder		
21	[30]	predetermined	Analytic Geometrical Method	Dual-System Cooperative co-evolutionary detecting Particle Swarm Optimization	4–60	Cuboid and Cylinder	2–29	Cuboid and Cylinder
22	[31]	-	developed PSO		1–40	Circle		
23	[32]	Genetic Algorithm (GA) and Tabu Search (TS)		differential evolution (DE)	2–19	Cuboid and Cylinder		
24	[33]	-	the Optimal Latin Hypercube (OLH) method	Nondominated Sorting Genetic Algorithm (NSGA)	Satellite Cabin-15	Cuboid and Cylinder		
25	[34]	equally allocated	Finite Circle Method (FCM)	developed PSO	2–18	Cylinder	2–16	Cuboid and Cylinder
26	[35]	equally allocated	Hybrid Differential evolution (DE) and gradient-based Sequential Quadratic Programming (SQP) for cylindrical shapes		2–14	Cylinder	2–40	Cylinder
27	[36]	a heuristic algorithm based on stepwise regression	a pseudo-algorithm employing differential evolution (DE)		4–60	Cuboid and Cylinder		
28	[37]	predetermined	Developed PSO and Phi-Function Method/FCM		4–60	Cuboid and Cylinder	2–16	Cuboid and Cylinder
29	[38]	equally allocated	Improved Niching Method (developed GA for cylindrical components)		2–14	Cylinder		

One of the essential constraints in satellite layout is the non-overlapping of components in all bearing plates, named layers. One common method is based on integrating Computer-Aided Design (CAD) tools, engineering analysis packages and optimization algorithms. Coupling optimization algorithms with Computer-Aided Design (CAD) and engineering analysis packages to find the optimal layout of spacecraft equipment was first proposed by [39]. After that, this method was applied in the studies of [22,23,26,33,40,41].

The following are the most important articles in the field of satellite equipment arrangement, and they present various methods in approaching the subject of non-overlapping.

For the first time, ref. [11] studied the arrangements of equipment on several satellite layers, and then analyzed the three-dimensional layout problem on a rotating vessel. Because of the spiral rotation movement of the vessel, they took into account dynamic equilibrium constraints and used the heuristic algorithms constructed by [42] for non-convex polygons to determine the amount of overlap among objects.

Sun, Z.G. et al. [12] introduced a centripetal balancing heuristic algorithm to allocate objects between bearing plates. To distribute objects in a bearing plate, they applied a Genetic Algorithm (GA) to produce random populations and finally to reach a feasible (near-optimal) solution. Eventually, they developed an Ant Colony Optimization (ACO) method to refine the positions of each object in a detailed design on bearing surfaces.

Huo, J. et al. [13] developed a human-guided GA, and compared its results with the GA library to demonstrate the efficacy of their algorithm for the two-dimensional layout of objects in a satellite. They added artificial individuals to the population of GA to cope with overlapping components.

Liu, Z. et al. [15] presented a Human–Algorithm–Knowledge approach with the support of GA to design the layout of equipment in a satellite, and used the CAD software to derive previous knowledge for use in their GA.

Zhang, B. et al. [1] developed a two-stage model for the layout optimization of satellites. The first stage concerned allocating objects to different bearing plates, and the second one dealt with the detailed design of each bearing plate such that no overlapping occurred. To develop an optimal layout in each bearing plate, they applied a combinatorial method including GA and Particle Swarm Optimization (PSO) metaheuristics. They explained that GA is inherently suited to finding global convergence, while PSO is the proper method for local convergence, and the disadvantage of GA in local convergence was compensated for using PSO to replace the random population in the initial phase of GA and the weakness of PSO in terms of global converge was satisfied using the best solution of GA to replace the first population of PSO. To tackle the overlapping issue, they applied the concept of the compaction and separation algorithm introduced by [43], who applied locality heuristics for star-shaped non-convex polygons.

Huo, J.Z. et al. [16] presented a co-evolutionary method in which a genetic algorithm (GA) was used to determine the rotation angle of the final layout scheme of the equipment, and a heuristic combination–rotation method was introduced to determine the entire layout scheme with reference to the rotation strategy of a heuristic constraint rubik cube method (CRCM).

Teng, H.F. et al. [20] proposed an evolutionary method called the dual-system variable-grain algorithm to decompose the satellite layout system into several sections, and also to avoid premature convergence problems. In their model, they took into account the constraints of interference between objects, the centroid offset of the satellite system and constraints of inertia angles. They applied analytic geometry to handle the discontinuous constraints related to overlapping volumes. Li, Z. et al. [27] presented a three-step strategy for distributing equipment throughout the layers of a satellite and then determining the location of each component inside its assigned layer. In the initial phase, each piece of equipment was assigned to one of the four bearing layers using a genetic algorithm (GA). In the second step, they applied a heuristic positioning rule to address the challenge of satisfying overlapping constraints between circles and rectangles in the precise 2D design of equipment for each layer. In this step, an ACO algorithm and a heuristic adjustment

approach are used to manage the detailed design of each layer. Lastly, they presented a PSO algorithm to combine subproblems and attempt to minimize errors in the mass center and moment of inertia, while preserving the other components of the objective function. Liu, J. et al. [25] proposed a hybrid method based on local and heuristic search algorithms to find the optimal arrangement of satellite equipment. They calculated the amount of equipment overlap based on geometric shapes. In this way, if two devices were rectangular, or one was rectangular and the other was circular, projection and no-fit polygon methods were used, respectively. The second method is utilized for the non-overlapping of polyhedra, in which all possible placements of a polyhedron in relation to others are illustrated, and the topic of overlapping between two polyhedra is relegated to overlapping between a polyhedron and a vector that is more computationally efficient. Cui, F.Z. et al. [30] represented a new dual algorithm combining the detecting of PSO and a cooperative co-evolution method for use in a multi-layer satellite. Similar to [20], here, analytic geometry was the method they proposed to deal with the problem of overlapping among components. Ref. [32] presented an integrated method for satellite equipment assignment and layout design. They used GA and Tabu Search (TS) to reassign equipment before attempting to lay out 19 components in two layers using the Differential Evolution (DE) method. Ref. [36] stated that the assignment of satellite equipment can be achieved based on the Multiple Bin Packing Problem (MBPP) approach. They offered a method based on stepwise regression to assign equipment, and after comparing the assignment schemes, the optimal one was chosen as the input for the layout phase, which was solved using a pseudo-algorithm employing DE and a random mutation operation. Refs. [37,44] evaluated the overlap between equipment in the satellite's central plane utilizing the method given in the paper by Chernov et al. (2012) [45] and the phi-function method. For two components, if the value of the phi-function is positive, the two components will not overlap; if the value of the function is zero, they are tangential to each other, and if it is negative, they intersect. Also, unlike most of the research done in this field, they here considered the interaction between the pieces of equipment. They studied five examples of different satellites. The first example involved six equilateral triangles in a circular enclosure, the second example involved resolving an overlapping problem between two diagonally placed rectangles, the third example concerned cylindrical satellites, the fourth example was for nano-satellites, and the final example concerned overlapping between parts in cube-shaped satellites. They solved the third and fifth instances using an adaptive PSO approach, and the fourth example using the Finite Circle Method (FCM), all of which were developed by [34]. Finally, the existing limitations associated with this method were also addressed, and it was shown that, due to the use of geometric non-linear and non-convex restrictions, the proposed model does not provide a sufficient solution for some conditions, and it is necessary that in the future, efficient and effective algorithms be produced to solve this problem.

In the field of uncertainty, defined uncertainty as the difference between the amount of information needed and the amount of information available to perform a task [46]. The uncertainty related to decision-making arises under conditions of incomplete information. Ref. [47] divided the discussion of uncertainty between issues of flexibility in limitations and the different levels of acceptability of goals, and those related to uncertainty in input data. In this way, the flexibility in the constraints takes into account the decision-maker's preferences. Ref. [48] divided decision-making conditions into two groups according to the quality of available information: decision-making under conditions of certainty (when information is fully available) and decision-making under conditions of uncertainty (when information is incomplete). Ref. [49] indicated that developments in robust optimization have taken place in three historical waves. The first wave, begun by [50], concerned robust optimization related to a scenario-based stochastic planning approach. Refs. [51,52] then developed this approach further. The second wave, known as robust convex programming, was first introduced by [53–55]. Here, the cone programming method is used to solve convex problems due to the existence of complexities, which is achieved according to duality theorems and optimality conditions. The third wave, pioneered by [56], presented

different approaches to robust planning. They demonstrated that robust fuzzy mathematical programming (RFMP) can be divided into two parts: possibilistic programming and flexible programming.

As the analyses in the literature demonstrate, there are two fundamental aspects to the satellite layout issue. First, there is the issue of component distribution across different bearing layers, and second, there is the problem of cuboid component overlapping. Accordingly, this paper addresses both problems.

In the next section, the mathematical modeling of satellite components' layout is described.

### 1.2. Mathematical Modeling

Conceptual design, preliminary design, and detailed design are the three basic stages of satellite design. One of the fundamental subjects of the detailed design phase is layout design, which encounters the issue of whether operational components from various subsystems can function properly and effectively when integrated in a unique environment, such as a space that is constantly exposed to cosmic rays.

The major goal of designing satellite equipment is to optimize a satellite's stability, control, and dimensions, which will result in a reduction in the size and weight of the satellite, and so this kind of optimization can have a direct impact on the satellite's launch success, as well as its continuity and durability in space.

Numerous factors, such as size, stability, and optimum system performance, contribute to the best satellite layout, and result in more variables and limitations. This intricacy emphasizes the need for industrial engineering optimization solutions rather than the typical trial-and-error methods used in mechanical engineering in this field. The challenge of placing many pieces of equipment in a cylinder, cube, or polygonal volume on different floors, and deploying multiple distinct plates within the satellite, is known as a problem related to optimizing telecommunication and measurement satellite equipment.

The layout optimization problem of a communication satellite module can be described as follows.

A total number of  $n$  components will be located in a cylindrical satellite module with two floors. Four plates, including the upper and lower and two middle plates of the inner space of the satellite, attached to a standing column in the module, are used to hold all the components, and in this proposed methodology, all the components are given simple cylindrical and cubic shapes and regarded as rigid bodies with uniform mass allocation.

There is an even distribution of mass across every piece of equipment, which are shaped as cubes or cylinders.

An extensive analysis of the influencing factors, such as distance constraints, heat constraints, radiation constraints, functional constraints, and stability, is crucial because the goal of this paper is to optimize the interior space of the satellite and ultimately reduce its dimensions and weight. The problem becomes more complex after a full analysis of these constraints, necessitating the employment of specialized optimization software. Therefore, the ultimate objective is to build an optimization model and ensure its output with the aid of software, so that manufacturing units can optimally place equipment when building satellites with smaller dimensions and weights.

The objective is to reduce the satellite's size and weight while still maintaining stability, taking into account the major inertia moments, cross-inertia moments, and center of gravity, as well as distance, heat, and radiation limits. The problem of equipment placement is an NP-hard problem because of the engineering and mechanical complexity of satellites. This calls for a combination of numerous intricate and specialized approaches, in addition to the design of a sophisticated system. For example, shown in Figure 1 is a typical cylindrical configuration of a satellite, with two center plates (or four layers/floors) for holding boxes and components across the satellite's multiple floors. The shape of the equipment is cylindrical or cubic, and all of it is located on one of the two sides of these center plates. As each side of a plate is called a layer, this satellite includes four layers. Depending

on the numbers, sizes and weights of the cylindrical and cubic boxes (representative of interior equipment of satellite), several solutions may be developed for the placement of the elements in the layers or floors of the satellite. Finding the optimum solution (i.e., the best layout or placement of elements, with the ability to satisfy the constraints of the problem) using optimization methods rather than trial-and-error methods is an interesting and important issue. Successful optimization methods can help the designers of satellites in reducing the time taken in designing the layout of the components and subsystems.

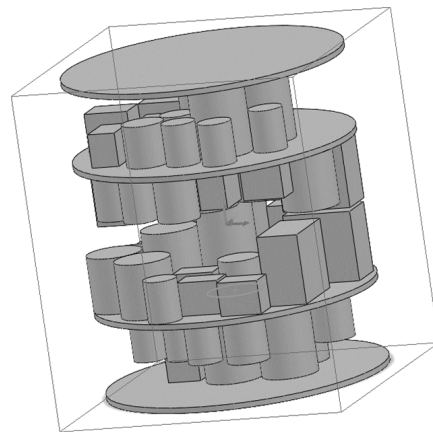


**Figure 1.** Example of the 3D layout of cubic or cylindrical components (boxes) of a sample satellite with two middle plates and four layers.

The assumptions of the model are as follows:

Three-dimensional layout—Difficulties in placing satellite equipment arise across three dimensions, so the Z axis is considered the main part;

Multi-layer layout—The multiple layers of a satellite represent another crucial consideration in the installation of satellite equipment. In relation to this, the model must allocate equipment to all plates or layers;

Non-interference and overlap constraints—No interference occurs between any pieces of the components;

Equilibrium constraint—The equilibrium error of the system should be as small as possible;

Thermal constraints—The performance of electronic components may be directly impacted by the thermal environment. As a result, the system's equipment is generally more efficient and reliable when heat flow is distributed uniformly.

From a thermal point of view, each piece of equipment has an effective area that can affect the performance of other equipment. Therefore, reducing the interaction space is essential to improving the uniformity of the thermal field in the satellite. In determining the thermal effects of equipment, it is assumed that some components produce a thermal radius that forms a uniform circle around the equipment. For this reason, no intersection between virtual thermal radii between equipment is allowed;

Obnoxious equipment limitations—Another constraint must be taken into account for some equipment types with a high amount of heat radiation, or "hot parts", such as batteries, radio transmitters, and photo transmitters, which must be positioned at as great a distance from one another as possible in the satellite space. In other words, there needs to be limitations placed on the presence of this hot equipment on each floor of the satellite;

Static stability constraint—The center of gravity offset of the system should be as small as possible.

The stability limit of the satellite should be such that the device can move and rotate easily in space. Therefore, the sum of the inertia moments of the system should be minimal. Physically, minimizing the sum of moments of inertia means that the satellite inherently

tends towards stability, and this minimization can reduce the effort required from subsystems in stabilizing the satellite, as a result of which moments of inertia, including the axes of the main axis and impact or cross moments, must be at a minimum.

**System uncertainty**—There is no fixed value for the distance at which equipment should be spaced apart, so it is important to use uncertainty to determine this distance. As mentioned in the previous section, uncertainties are included in the model for a variety of reasons—one of them is uncertainty on the part of the decision-maker (DM). In the design of satellite equipment layout, it is not easy to apply non-overlap constraints to cube-shaped equipment with a rectangular cross-section as has been done for cylindrical equipment with a circular cross-section, because, when there are two items of circular equipment, the overlap between them can be easily prevented by calculating the radius and entering the distance between the two radii. On the other hand, for two pieces of equipment with a rectangular cross-section, or when there is one piece of circular equipment and another rectangular one, the non-overlap restriction cannot be easily observed. For this reason, the uncertainty argument is easily applicable, and is very effective in developing a solution.

Due to the nature of the problem, the fuzzy concept is also used here, meaning that the constraints related to equipment distances are written in fuzzy form. By adding fuzzy constraints, a decision variable ( $\alpha$ ) is defined in the model and added to the objective function with a penalty coefficient ( $\gamma$ ).

### 1.2.1. Model Development

In this section, we outline the parameters, decision variables, objective functions and constraints of the basic model, derived from previous studies such as [1,12,15] and to be utilized for introducing and defining the 3D layout problem, and the optimization method is also illustrated.

#### Model Parameters

The model parameters are introduced as follows:

$i$ —indicator of the equipment;

$j$ —index of the number of layers ( $j = 1, 2, 3, 4$ )

$l_j$ —layer  $j$  of the satellite;

$a_i$ —the cross-sectional length of the cuboid equipment  $i$ ;

$b_i$ —the cross-sectional width of the cuboid equipment  $i$ ;

$r_i$ —radius of the cross-sectional area of the cylindrical equipment  $i$ ;

$h_i$ —the height of the equipment  $i$ ;

$m_i$ —the mass of equipment  $i$ ;

$\theta_i$ —the angle between the positive direction of the  $x$ -axis and the horizontal edge of the cuboid equipment  $i$ ;

$c$ —number of pieces of cuboid equipment;

$n$ —total number of equipment;

$n_j$ —the number of equipment pieces located at layer  $j$ ;

$sM_i$ —a segment of the radius of the hypothetical circumferential circle of a cross-section of cuboid equipment  $i$ ;

$sO_i$ —optimistic value of a triangular fuzzy number for  $sM_i$ ;

$sP_i$ —pessimistic value of a triangular fuzzy number for  $sM_i$ ;

$\tilde{sT}_i$ —a triangular fuzzy number for  $sM_i$ ;

$\gamma$ —the cost of the fine for each unit of violation of the soft limit;

$x_e$ —expected coordinates in the direction of the  $x$ -axis of the satellite's center of gravity;

$y_e$ —expected coordinates in the  $y$ -axis direction of the satellite's center of gravity;

$z_e$ —expected coordinates in the direction of the  $z$ -axis of the satellite's center of gravity;

$J_{xi}$ —moment of inertia of equipment in the direction of the  $x$ -axis;

$J_{yi}$ —moment of inertia of equipment in the direction of the  $y$ -axis;

$J_{zi}$ —moment of inertia of equipment in the direction of the  $z$ -axis;

$\delta x_e$ —permissible error of deviation in the coordinates of the real center of gravity of the satellite from the expected value in the direction of the  $x$ -axis;  
 $\delta y_e$ —permissible error of deviation in the coordinates of the real center of gravity of the satellite from the expected value in the direction of the  $y$ -axis;  
 $\delta z_e$ —permissible error of deviation in the coordinates of the real center of gravity of the satellite from the expected value in the direction of the  $z$ -axis;  
 $\delta\theta_x$ —permissible error of deviation in the angle between the mass moment of inertia of the satellite in the direction of the  $x$ -axis from the axis of the coordinate of the satellite in the direction of the  $ox$  axis;  
 $\delta\theta_y$ —permissible error of deviation in the angle between the mass moment of inertia of the satellite in the direction of the  $y$ -axis and the axis of the satellite coordinates in the direction of the  $oy$  axis;  
 $\delta\theta_z$ —permissible error of deviation in the angle between the mass moment of inertia of the satellite in the direction of the  $z$ -axis from the coordinate axis of the satellite in the direction of the  $z$ -axis.

#### Decision Variables of the Model

The model's decision variables are as follows:

$x_i$ —the coordinates of equipment  $i$  in the direction of the  $x$ -axis;  
 $y_i$ —the coordinates of equipment  $i$  in the direction of the  $y$ -axis;  
 $z_i$ —the coordinates of equipment  $i$  in the direction of the  $z$ -axis;  
 $x_m$ —coordinates of the center of gravity of the satellite in the direction of the  $x$ -axis;  
 $y_m$ —the coordinates of the center of gravity of the satellite in the direction of the  $y$ -axis;  
 $z_m$ —coordinates of the center of gravity of the satellite in the direction of the  $z$ -axis;  
 $\theta_x$ —the angle between the mass moment of inertia of the satellite in the direction of the  $x$ -axis and the axis of the satellite coordinates in the direction of the  $x$ -axis;  
 $\theta_y$ —the angle between the mass moment of inertia of the satellite in the direction of the  $y$ -axis and the coordinate axis of the satellite in the direction of the  $y$ -axis;  
 $\theta_z$ —angle between the mass moment of inertia of the satellite in the direction of the  $z$ -axis and the axis of coordinates of the satellite in the direction of the  $oz$  axis;  
 $I_{xx}$ —the mass moment of inertia of the satellite in the direction of the  $x$ -axis;  
 $I_{yy}$ —the mass moment of inertia of the satellite in the direction of the  $y$ -axis;  
 $I_{zz}$ —the mass moment of inertia of the satellite in the direction of the  $z$ -axis;  
 $I_{xy}$ —product moment of inertia used to calculate satellite imbalance in the direction of the  $x$  and  $y$  plane;  
 $I_{xz}$ —product moment of inertia used to calculate satellite imbalance in the  $x$  and  $z$  plane directions;  
 $I_{yz}$ —product moment of inertia used to calculate satellite imbalance in the  $y$  and  $z$  plane directions;  
 $fr_i$ —the final radius of equipment  $i$  after performing the uncertainty calculations;  
 $\alpha_i$ —the minimum level of satisfaction in flexible constraints;  
 $S_j$ —the space available on each layer;  
 $S'_j$ —the space occupied on each layer.

There are three types of coordinate systems:

#### 1. $Oxyz$ reference coordinate system

$O$ —the center of this coordinate system is located on the geometric center of the lower plate of the satellite;  
 $z$ —the longitudinal symmetric axis of the satellite, which is positive in the upward direction;  
 $x$ —the axis perpendicular to the  $z$ -axis on the bottom plate of the satellite;  
 $y$ —the axis perpendicular to the  $z$ -axis on the bottom plate of the satellite and at a 90-degree angle to the  $x$ -axis.

This coordinate system is used to find the center of the satellite and determine the layout of the equipment.

2. Satellite coordinate system  $O'x'y'z'$

$O'$ —the center of this coordinate system is located on the real center of gravity of the satellite.

$z'$ —the longitudinal symmetric axis of the satellite that coincides with or is parallel to the  $z$ -axis.

$x', y'$ —these two axes are parallel to the  $x$ - and  $y$ -axes, respectively.

This coordinate system is used to calculate the mass and product moment of inertia of the satellite.

3. The local coordinate system of the equipment  $O''x''y''z''$

$O''$ —the center of this coordinate system is located on the center of gravity of the equipment;

$z''$ —the longitudinal symmetric axis of the equipment, which is parallel to the  $z$ -axis.

$x'', y''$ —these two axes form an angle  $\alpha_i$  parallel to the  $x$ - and  $y$ -axes, respectively.

This coordinate system is used to calculate the moment of inertia of the equipment according to its axis.

Optimization Model

A minimal sum of the moments of inertia physically suggests that the satellite is inherently stable. This means that minimizing the sum of the moments of inertia can reduce the efforts required from the attitude control subsystem in the stabilization of the satellite.

The moments of inertia of both cubic and cylindrical components are calculated in the  $xyz$  direction. The total moments of inertia of all the components that need to be minimized can be expressed as follows:

$$\text{Min } f(X) = I_{xx} + I_{yy} + I_{zz} \tag{1}$$

The constraints are as below.

Non-overlap constraint:

$$g_1(X) = -(x_i - x_j)^2 - (y_i - y_j)^2 + (r_i + r_j)^2 \leq 0 \text{ for } i, j \in L_k \quad k = 1, 2, 3, 4 \tag{2}$$

Static stability constraint:

$$g_2(X) = |x_m - x_e| - \delta x_e \leq 0 \tag{3}$$

$$g_3(X) = |y_m - y_e| - \delta y_e \leq 0 \tag{4}$$

$$g_4(X) = |z_m - z_e| - \delta z_e \leq 0 \tag{5}$$

where  $x_e, y_e$  and  $z_e$  are the expected centroid position of the satellite and  $\delta x_e, \delta y_e$  and  $\delta z_e$  are the allowance errors of  $x_m, y_m$  and  $z_m$  (real centroid position of the satellite), respectively.

Equilibrium constraints:

$$g_5(X) = |\theta_x - \theta_e| - \delta \theta_x \leq 0 \tag{6}$$

$$g_6(X) = |\theta_y - \theta_e| - \delta \theta_y \leq 0 \tag{7}$$

$$g_7(X) = |\theta_z - \theta_e| - \delta \theta_z \leq 0 \tag{8}$$

where  $\theta_x, \theta_y$  and  $\theta_z$  are angles between the principal axes of inertia of the satellite and the principle axes  $oz, oy$  and  $oz$ , and  $\delta \theta_x, \delta \theta_y$  and  $\delta \theta_z$  are their allowance errors.

The objective function (1) shows the minimization of mass moments of inertia in the main direction of the coordinate axis. Constraint (2) represents the constraint of non-overlapping between pieces of equipment by requiring that the distance between the centers of two pieces of equipment be equal to or larger than the sum of their two radii. For cuboid equipment, the radius of the circumferential circle of the rectangular cross-section is considered as the radius.

Constraints (3) to (5) show static stability, where  $x_e, y_e$  and  $z_e$  coordinates are the expected center of gravity of the satellite and  $\delta x_e, \delta y_e$  and  $\delta z_e$  are permissible error in the coordinates of the actual center of gravity of the satellite ( $x_m, y_m, z_m$ ). The deviation of the center of gravity of the satellite after the placement of all equipment should not be greater than that in the expected center of gravity of the satellite. Constraints (6) to (8) are equilibrium constraints, in which  $\theta_x, \theta_y$  and  $\theta_z$  are the angles between the directions of the mass moments of inertia of the satellite with the major axes  $O_x, O_y$  and  $O_z$ , and  $\delta\theta_x, \delta\theta_y$  and  $\delta\theta_z$  are their allowable errors. The following shows how to calculate  $\theta_x, \theta_y$  and  $\theta_z$ .

The center of mass of the  $i$ th component in the local  $xyz$  coordinate system can be stated as shown below:

$$x_m = \sum_{i=1}^n m_i x_i \div \sum_{i=0}^n m_i \tag{9}$$

$$y_m = \sum_{i=1}^n m_i y_i \div \sum_{i=0}^n m_i \tag{10}$$

$$z_m = \sum_{i=1}^n m_i z_i \div \sum_{i=0}^n m_i \tag{11}$$

where  $(x_i, y_i, z_i)$  and  $m_i$  are the coordinates of the center and the mass of the piece of equipment  $i$ , respectively. In the denominator of these equations, the sum starts from zero because, in addition to the number of pieces of equipment ( $n$ ), the mass of the shell, the middle cylinder and the floors must also be taken into account in calculating the true center of gravity of the satellite.

The computational formulas of moments of inertia in the main directions of the satellite coordinate axis are as follows:

$$\begin{aligned} I_{xx} &= \sum_{i=1}^n (J_{xi} \cos^2\theta_i + J_{yi} \sin^2\theta_i) + \sum_{i=1}^n m_i (y_i^2 + z_i^2) - \sum_{i=0}^n m_i (y_m^2 + z_m^2) \\ &= \sum_{i=1}^c (\frac{1}{12} (m_i (b_i^2 + h_i^2) \cos 2\theta_i + \frac{1}{12} m_i (a_i^2 + h_i^2) \sin 2\theta_i) \\ &\quad + \sum_{i=c+1}^n \frac{1}{12} m_i (3r_i^2 + h_i^2) + \sum_{i=1}^n (m_i (y_i^2 + z_i^2) - \sum_{i=0}^n (m_i (y_m^2 + z_m^2)) \end{aligned} \tag{12}$$

where  $J_{xi}$  and  $J_{yi}$  are moments of inertia of the  $i$ th component concerning the local coordinate system (to the  $x$ - and  $y$ -axes, respectively).  $a_i$  and  $b_i$  are the length and width of a cubic component, respectively, and  $h_i$  and  $r_i$  are the height and radius of the  $i$ th component (for both cubic and cylindrical components). Similarly, the derivations of moments of inertia in the  $y$  direction of both cylindrical and cubic components are shown below:

$$\begin{aligned} I_{yy} &= \sum_{i=1}^c (\frac{1}{12} m_i (a_i^2 + h_i^2) \cos^2\theta_i + \frac{1}{12} m_i (b_i^2 + h_i^2) \sin^2\theta_i) + \sum_{i=c+1}^n \frac{1}{12} m_i (3r_i^2 + h_i^2) \\ &\quad + \sum_{i=1}^n (m_i (x_i^2 + z_i^2) - \sum_{i=0}^n (m_i (x_m^2 + z_m^2)) \end{aligned} \tag{13}$$

Similarly, the derivations of moments of inertia in the  $z$  direction of both cylindrical and cubic components are illustrated below:

$$I_{zz} = J_{zi} + \sum_{i=1}^n m_i (x_i^2 + y_i^2) - \sum_{i=0}^n m_i (x_m^2 + y_m^2) \tag{14}$$

$\alpha_i$ —this parameter is the placement angle of the cubic object; it equals the included angle between axis  $x$  in the positive direction and the long edge of the cubic component. Here, it is assumed that the cubic equipment only rotates 90 degrees, so the only possible values for this parameter are zero or 90.

The formulae of  $\theta_x$ ,  $\theta_y$  and  $\theta_z$  are as below:

$$\theta_x(x) = \arctan \frac{2I_{xy}}{I_{xx} - I_{yy}} \tag{15}$$

$$\theta_y(x) = \arctan \frac{2I_{xz}}{I_{zz} - I_{xx}} \tag{16}$$

$$\theta_z(x) = \arctan \frac{2I_{yz}}{I_{zz} - I_{yy}} \tag{17}$$

where  $I_{xy}$ ,  $I_{xz}$  and  $I_{yz}$  are the products of moments of inertia in the  $x - y$ ,  $x - z$  and  $y - z$  planes, respectively, for both cylindrical and cubic components, and are calculated as below:

$$\begin{aligned} I_{xy} &= \sum_{i=1}^n (m_i(x_i - x_m)(y_i - y_m) + (J_{xi} + (y_i^2 + z_i^2) - J_{yi} - (x_i^2 + z_i^2)) \div 2) \times \sin 2\theta_i \\ &= \sum_{i=1}^n \left[ m_i x_i y_i + \frac{J_{xi} + m_i(y_i^2 + z_i^2)}{2} \sin 2\theta_i \right] \\ &\quad - \sum_{i=1}^n \left[ \frac{J_{yi} + m_i(x_i^2 + z_i^2)}{2} \sin 2\theta_i \right] - \sum_{i=1}^n m_i x_m y_m \end{aligned} \tag{18}$$

$$I_{xz} = \sum_{i=1}^n (m_i(x_i - x_m)(z_i - z_m)) = \sum_{i=1}^n m_i x_i z_i - \sum_{i=1}^n m_i x_m z_m \tag{19}$$

$$I_{yz} = \sum_{i=1}^n (m_i(y_i - y_m)(z_i - z_m)) = \sum_{i=1}^n m_i y_i z_i - \sum_{i=1}^n m_i y_m z_m \tag{20}$$

The moments of inertia of the  $i$ th cylindrical component are defined by  $J_{xi}$ ,  $J_{yi}$  and  $J_{zi}$  in relation to the local coordinate system, as follows:

$$J_{xi} = J_{yi} = \frac{1}{12} m_i (3r_i^2 + h_i^2) \tag{21}$$

$$J_{zi} = \frac{1}{2} m_i r_i^2 \tag{22}$$

Also, moments of inertia for the  $i$ th cubic component indicated by  $J_{xi}$ ,  $J_{yi}$  and  $J_{zi}$  are shown below:

$$J_{xi} = \frac{1}{12} m_i (b_i^2 + h_i^2) \tag{23}$$

$$J_{yi} = \frac{1}{12} m_i (a_i^2 + h_i^2) \tag{24}$$

$$J_{zi} = \frac{1}{12} m_i (a_i^2 + b_i^2) \tag{25}$$

## 2. Problem Statement and Implementation

The main issue to be investigated in this study is how to deal with the component assignment problem, along with the growing number of bearing layers and components and the complexity of technical requirements related to the satellite layout problem. In this

section, we offer a heuristic solution for the assignment problem, and then the RFMP is used to evolve the distance between cuboid components.

In approaching the mentioned problem, consider Figure 2, which shows the front view of a satellite in which components and boxes (cylindrical or cubic parts) are located on two floors or four layers (levels), such that the equipment is located on the upper and lower levels of each floor. The center of gravity of the satellite shown in Figure 2 ( $x_m, y_m, z_m$ ) is somewhere between levels  $L_2$  and  $L_3$  (i.e., between the two middle plates of the satellite). The distance between the layers and the bottom plate of the satellite is defined by  $H_1$ ,  $H_2$  and  $H_t$  as shown in Figure 2. The parameters introduced in Figure 2 will be explicated in the next part.

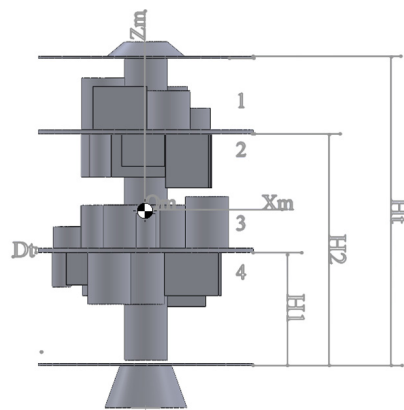


**Figure 2.** Front view of satellite with two middle plates and the locations of components in four layers.

### 2.1. Allocation and Layout

The placement of equipment in the satellite space involves two main steps: first, the allocation of equipment to floors and layers, and then their placement in each layer. As such, the problem is one of allocation and layout. Since the objective function involves minimizing mass moments of inertia, the equipment should be arranged such that the moments of inertia possess the lowest possible values in all directions of the coordinate axes ( $x, y, z$ ). Since the problem involves two floors and four layers, the placement of equipment can affect the moments of inertia in two ways.

The location of equipment at different levels affects the moment of inertia in the directions of the  $x$ - and  $y$ -axes, and the layout of the equipment at each layer can affect the moment of inertia in the direction of the  $z$ -axis ( $I_{zz}$ ). In other words, to change the moment of inertia in the directions of the  $x$ - and  $y$ -axes, the distances of the pieces of equipment from the  $o_m x_m$  and  $o_m y_m$  axes, respectively, play a decisive role. Therefore, if a component is moved between layers, its distance from the mentioned axes changes, and this affects the moment of inertia in the  $x$  and  $y$  directions. Conversely, if the distance of the equipment from the  $o_m z_m$  axis remains constant, there will be no change in the moment of inertia in the direction of the  $z$ -axis. According to this, the proper allocation of equipment to different layers can play an important role in reducing the moment of inertia in the directions of the  $x$ - and  $y$ -axes ( $I_{xx}$  and  $I_{yy}$ ).

#### 2.1.1. Allocation of Components between Layers

At this stage, all components are assigned to one of four layers in the satellite such that the most optimal state is created for the intended function. As previously explained, the assignment of equipment to surfaces can affect the moments of inertia along the  $x$ - and  $y$ -axes ( $I_{xx}$  and  $I_{yy}$ ). Since Equations (12) and (13) are similar, calculations are here only undertaken for one of them, and the result is generalized to the other. As is evident from Equation (26), to obtain the lowest possible value for this expression, the first three

expressions must show the lowest value, and the last expression must have the maximum possible value.

$$\sum_{i=1}^c (\frac{1}{12}m_i(b_i^2 + h_i^2)\cos^2\theta_i + \frac{1}{12}m_i(a_i^2 + h_i^2)\sin^2\theta_i) + \sum_{i=c+1}^n \frac{1}{12}m_i(3r_i^2 + h_i^2) + \sum_{i=1}^n (m_i(y_i^2 + z_i^2)) - \sum_{i=0}^n (m_i(y_m^2 + z_m^2)) \tag{26}$$

Before considering the minimization of the above expression, we must first discuss the value of  $z_i$ . This value indicates the final localization of the equipment in terms of height (z dimension) after placement. This is calculated as follows:

$$z_i = \begin{cases} H_2 + D_t + \frac{h_i}{2} & \text{if } l_j = 1 \\ H_2 - \frac{h_i}{2} & \text{if } l_j = 2 \\ H_1 + D_t + \frac{h_i}{2} & \text{if } l_j = 3 \\ H_1 - \frac{h_i}{2} & \text{if } l_j = 4 \end{cases} \tag{27}$$

Since the length, width and height ( $a, b, h$ ) of cuboid equipment, and the radius and height ( $r, h$ ) of cylindrical equipment, are fixed, the first three expressions of Equation (26) cannot be altered. Therefore, to change the equation, we must perform the following:

$$\sum_{i=1}^n (m_i(y_i^2 + z_i^2)) - \sum_{i=1}^n (m_i(y_m^2 + z_m^2)) \tag{28}$$

First, we consider the first part of the above equation. Given that the allocation of equipment to distinct layers impacts their z-axis coordinates, it suffices to minimize the first half of Formula (28) to minimize the following value:

$$\sum_{i=1}^n (m_i z_i^2) \tag{29}$$

We now turn to the second part of Equation (28). According to Equations (10) and (11), which concern the coordinates of the center of mass in the directions of the axes  $y$  and  $z$ , the second expression of Equation (28) is written as follows:

$$\sum_{i=1}^n (m_i (\sum_{i=1}^n m_i y_i \div \sum_{i=1}^n m_i)^2 + m_i (\sum_{i=1}^n m_i z_i \div \sum_{i=1}^n m_i)^2) \tag{30}$$

As can be observed, the denominator of both fractions in Formula (30) is the sum of the mass of all the equipment, which is a constant and can be omitted from the maximization computation. On the other hand, since in this part, the layout of equipment in each layer is not considered, and only their locations are important to the surfaces, we can omit the first part of (30), which refers to the coordinates in the direction of the  $y$ -axis. It is thus sufficient to maximize the following value to maximize the whole expression:

$$\sum_{i=1}^n (m_i) (\sum_{i=1}^n m_i z_i)^2 \tag{31}$$

Since the total mass of all equipment is a fixed value, the only part that will need to be maximized is as follows:

$$(\sum_{i=1}^n m_i z_i)^2 \tag{32}$$

Here, there are two expressions (29) and (31). One should take the maximum possible value, and the other should be minimized:

$$\text{Min} \sum_{i=1}^n (m_i z_i^2) \text{ and } \text{Max} (\sum_{i=1}^n m_i z_i)^2 \tag{33}$$

As is known, maximizing the expression  $(\sum_{i=1}^n m_i z_i)^2$  is equivalent to maximizing  $\sum_{i=1}^n m_i z_i$ , but in the first expression, the minimization of  $\sum_{i=1}^n m_i z_i^2$  is considered. Therefore, as the second power in the expression of minimization indicates, this part is of higher priority than the part regarding maximization, and in principle, the heavier the mass of the equipment at lower layers, the lower the product of mass in their height will be, and so the total moment of inertia in the direction of the  $x$ -axis ( $I_{xx}$ ) will assume the lowest possible value.

On the other hand, according to Equation (11) and considering that the moment of inertia is calculated according to the coordinates of the center of gravity, it can be concluded that the closer the equipment is to the center of gravity of the satellite, the lower the moment of inertia in the direction of the  $x$ -axis ( $I_{xx}$ ) and  $y$  ( $I_{yy}$ ) will be. Therefore, it makes sense to place more equipment in the middle layers (layers  $L_2$  and  $L_3$ ) so as to minimize the moment of inertia. According to the above explanations, we conclude that, in order to optimize the allocation of equipment at different levels of the satellite, it is best to place heavier equipment at lower layers ( $L_3$  and  $L_4$  layers) and to group more items in the middle layers (layers  $L_2$  and  $L_3$ ). Now, to satisfy the abovementioned cases, the following heuristic method is presented.

#### Heuristic Method to Allocate Equipment to Different Layers

Step 1: Arrange all the equipment at the same time based on height ( $h$ ) and mass ( $m$ ). Since all equipment is symmetrical and the mass distribution is assumed to be the same, the center of mass of each item of equipment is located in the middle, and its height is equal to half the height of the equipment ( $\frac{h}{2}$ ). Therefore, pieces of equipment that have a lower height are prioritized for placement in the initial and final layer (layers  $L_1$  and  $L_4$ ). Conversely, if the height of the equipment is great, placing it in one of the middle layers (layers  $L_2$  and  $L_3$ ) will reduce the distance between it and the center of gravity of the satellite, thus decreasing the moment of inertia along the  $x$ -axis ( $I_{xx}$ ) and  $y$ -axis ( $I_{yy}$ ).  
 Step 2: The space available on each layer is displayed by  $S_j$ , and variable  $S'_j$  refers to the amount of layer  $j$  occupied by the equipment. If more than 70% of the area on each layer ( $0.7 \times S_j$ ) is occupied by equipment, localization here will be practically impossible, as it will not be possible to place the equipment without overlapping. Moreover, since the area occupied by the equipment at levels  $L_2$  and  $L_3$  must be at least two times the area occupied by the equipment on layers  $L_1$  and  $L_4$ , the following ratio forms between the surface areas:

$$2 \times (S'_1 + S'_4) \leq S'_2 + S'_3 \leq 1.4 \times (\frac{1}{S' - 1.4}) \times (S'_1 + S'_4) \tag{34}$$

where

$$S' = \sum_{j=1}^4 S'_j \tag{35}$$

Step 3: After the equipment is arranged according to height and mass, to minimize the moments of inertia, pieces of equipment with lower heights should be placed on layers  $L_1$  and  $L_4$ , and to satisfy Equation (22), the equipment with the lowest height and mass values will be selected and placed on a list called A. This separation is necessary so that this equipment can be assigned to the two layers  $L_1$  and  $L_4$ , and the rest of the equipment will be automatically assigned to layers  $L_2$  and  $L_3$ . An approximate value means that one can start from Equation (36) to satisfy Equation (34) and return to this step to add the next piece of equipment to List A if the final assignment of Equation (34) is not met.

$$(S'_1 + S'_4) \geq S' - 1.4 \tag{36}$$

where  $S'$  is the total area available for the equipment in the four layers. There are only a few cases in which Equations (34) and (36) are met. For example, if there are a total of 60 pieces of equipment, and it is determined by the initial division that only in cases where  $n_1 + n_4 = 19, 20, 21$  or  $22$  does the ratio of Equation (22) remain eligible, then the following steps will be performed for the feasible cases.

Step 4: The selected equipment (List A) that makes up  $n_1 + n_4$  is sorted by mass from low to high.

Step 5: To allocate equipment to layer  $L_1$ , start from the lowest height and the lowest amount of mass and work up until the following ratio of the total area of the selected equipment becomes feasible,

$$0.4 (S'_1 + S'_4) \leq S'_1 \leq 0.6 (S'_1 + S'_4) \tag{37}$$

This division is intended to maintain the balance of equipment between the first and fourth layers. Therefore, with the first choice that satisfies this ratio, the allocation of equipment to the first level is completed, and the values of  $n_1$  and  $S'_1$  are determined.

Step 6: The rest of the equipment is assigned to layer  $L_4$ , and the values of  $n_4$  and  $S'_4$  are determined.

Step 7: The rest of the equipment (remaining about  $\frac{2}{3}$ ), which makes up  $n_2 + n_3$ , should be assigned to the two layers  $L_2$  and  $L_3$ . Accordingly, the equipment is ordered by height and then mass, from the greatest to the lowest value;

Step 8: Since, according to the previous description, the equipment must occupy less than 70% of the area of each layer, the remaining equipment will be assigned to the two layers  $L_2$  and  $L_3$  in such a way that the components are again arranged from the lowest to the highest value, and assigned to layer  $L_2$  until the following ratios are met, after which the remaining equipment is assigned to layer  $L_3$ .

$$S'_2 \leq 0.7S_2 \tag{38}$$

$$S'_3 \leq 0.7S_3 \tag{39}$$

$$0.9S'_3 \leq S'_2 \leq 1.1S'_3 \tag{40}$$

According to the previously mentioned constraints, such as Equation (33), and the need for a balanced distribution of equipment between layers, following the completion of Equations (38) and (39), Equation (40) must also be performed with relation to these two layers. Thus, all equipment is assigned to all layers, with heavier equipment placed on layers  $L_3$  and  $L_4$ , and equipment with the lowest height on layers  $L_1$  and  $L_4$ .

Step 9: Upon completion of equipment allocation, the information obtained should be placed in the GAMS software (v.24.1.3), following which the problem can be considered initially solved, and the optimal local solution will be generated and stored. The assigning of an initial solution means that uncertainty is not considered at this point, and the designing of a detailed layout with equipment on each floor is done in the next section. By employing the presented heuristic method, all the cases that may produce a near-optimal solution are considered, and the best arrangements are used as inputs in the next stage.

### 2.1.2. Layout of Equipment in Each Layer

Since the satellite's components are cuboid or cylindrical, they can be viewed in two dimensions as a rectangle or a circle. To satisfy the non-overlap constraint between equipment, the location of each piece of equipment must be compared with the locations of others, and no overlap between any components will be allowed. Here, two types of survey are required: one for circular cross-sectioned equipment and one for rectangular cross-sectioned equipment.

Satisfying the non-overlap constraint for equipment with a circular cross-section is easily achievable. To do this, it is sufficient to rewrite constraint number 2, as follows.

$$(r_i + r_j)^2 \leq (x_i - x_j)^2 + (y_i - y_j)^2 \tag{41}$$

As indicated by the inequality in (41), the Euclidean distance between the centers of both circles must be greater than or equal to the sum of the radii of the two circles.

For equipment with a rectangular cross-section, satisfying the non-overlap constraint is not as simple as it is with circular equipment. In this article, we use flexible and robust programming to solve this problem. It is assumed that each rectangle can be represented by a circle whose center is positioned in the same location as the center of the rectangle, and after this, no overlap between these circles is allowed.

Now, if the abovementioned circle is considered as a circumscribed rectangular circle, satisfying the non-overlap constraint will increase the distance between the pieces of equipment more than is necessary, and as a result, the objective function will degrade. If the circle is designed to be so small that it becomes inscribed on the rectangle, then even though the objective function is greatly reduced and the components are positioned at shorter distances from each other, we will see the overlap of parts of the rectangular components, and the non-overlap constraint will be violated.

Therefore, it is essential to find virtual circles that, while satisfying the non-overlap constraint, can present optimal and minimal values of the objective function. To achieve the best hypothetical circle, a novel approach is applied. As shown in Figure 3, the value of  $sM$  is considered as a parameter to determine the optimal radius of the hypothetical circle. Other parameters (i.e.,  $r$ ,  $x$  and  $y$ ) have also been defined previously.

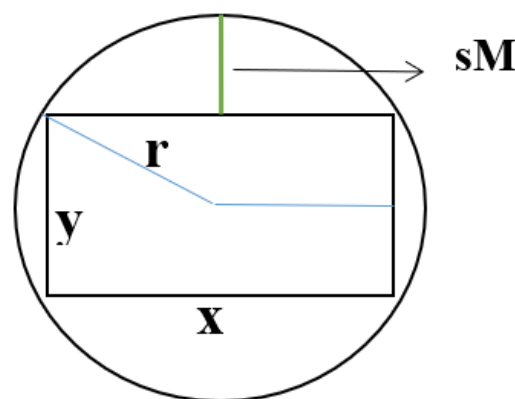


**Figure 3.** Defining the circle circumscribed for equipment with a rectangular cross-section in terms of  $sM$ , dimensions of the rectangle ( $x, y$ ) and the radius of the circle ( $r$ ).

If the hypothetical circle displayed the largest radius and we converted the circumscribed circle to a rectangle, the value of  $sM$  could be calculated as follows

$$sM_i = r(i) - \frac{\min(x(i),y(i))}{2} \tag{42}$$

where  $x$  and  $y$  are the length and width of the rectangle, respectively, and  $r$  is the radius of its hypothetical circumscribed circle.

Conversely, if the radius of the hypothetical circle is the smallest, and is set out as a circle inscribed in the rectangle, the value of  $sM$  will tend to be zero. To ensure a flexible constraint and a robust concept, fuzzy numbers are an appropriate option, because the nature of fuzzy numbers closely affects flexible robust programming [49].

2.2. Robust Flexible Programming Model (RFPM)

To cope with the difficulties associated with overlapping issues for rectangle shapes, a robust flexible programming model is proposed.

Based on the RFPM introduced by [49], fuzzy numbers are represented as triangular numbers in this paper.

To solve the problem using flexible programming, the model is first written as follows:

$$\text{Min } f(x) = I_{xx} + I_{yy} + I_{zz} \tag{43}$$

s.t.

$$fr_i \overset{\sim}{\geq} r_i \quad i \in \text{cubic equipments} \tag{44}$$

$$fr_i \geq r_i \quad i \in \text{cylinder equipments} \tag{45}$$

$$(fr_i + fr_{i+1})^2 \leq (x_i - x_{i+1})^2 + (y_i - y_{i+1})^2 \quad i \in \text{cubic equipments} \tag{46}$$

The sign of  $\overset{\sim}{\geq}$  represents the fuzzy version of  $\geq$ , and illustrates that the value of the right hand side of the constraint is smaller than or similar to that of the left hand side. The fuzzy number  $\overset{\sim}{sT}$  can be used to depict the flexible condition of the fuzzy constraint.

Therefore, the model can be rewritten as follows:

$$\text{Min } f(x) = I_{xx} + I_{yy} + I_{zz} \tag{47}$$

s.t.

$$fr_i \geq r_i - \overset{\sim}{sT} \times (1 - \alpha_i) \quad i \in \text{cubic equipments} \tag{48}$$

$$fr_i \geq r_i \quad i \in \text{cylinder equipments} \tag{49}$$

$$(fr_i + fr_{i+1})^2 \leq (x_i - x_{i+1})^2 + (y_i - y_{i+1})^2 \quad i \in \text{cubic equipments} \tag{50}$$

The  $\alpha$  parameter indicates a minimum level of satisfaction with the flexible constraint. Suppose that the fuzzy number  $\overset{\sim}{sT}$  is a triangular fuzzy number represented by three numbers ( $\overset{\sim}{sT} = (sP.sM.sO)$ ), which can be elucidated by the method demonstrated in Yager (1981) as follows:

$$\overset{\sim}{sT} = \left( sM + \frac{(sO - sM) - (sM - sP)}{3} \right) \tag{51}$$

Based on constraint 2, the flexible programming model can be rewritten in the non-fuzzy mode as follows:

$$\text{Min } f(x) = I_{xx} + I_{yy} + I_{zz} \tag{52}$$

s.t.

$$fr_i \geq r_i - sMi + \left( \frac{(sO - sM) - (sM - sP)}{3} \right) \times (1 - \alpha_i) \quad i \in \text{cubic equipments} \tag{53}$$

$$fr_i \geq r_i \quad i \in \text{cylinder equipments} \tag{54}$$

$$(fr_i + fr_{i+1})^2 \leq (x_i - x_{i+1})^2 + (y_i - y_{i+1})^2 \quad i \in \text{cubic equipments} \tag{55}$$

The expression  $\left( \frac{(sO - sM) - (sM - sP)}{3} \right) \times (1 - \alpha_i)$  indicates the permissible amount of violation of the flexible constraint. It should be noted that the use of this flexible fuzzy programming method allows other fuzzy numbers to be used in the fuzzy constraint, and

other fuzzy ranking methods can also be used to de-fuzzy the uncertain parameters present in the soft constraints.

Also, using  $\alpha$ -cuts to determine the degree of violation in soft constraints can lead us to different fuzzy solutions that help decision-makers in comparing different outputs and achieving better solutions in sensitivity analysis.

In the fuzzy flexible planning model, the decision of whether to allocate the lowest level of satisfaction to the flexible constraints ( $0 \leq \alpha \leq 1$ ) must be made by the decision-maker. In other words, this method should be reactive, and the decision-maker will achieve different results by manually changing the minimum level of satisfaction and extracting the best solutions for the fuzzy parameters.

The desirability of choices made at each stage is determined by the output of the model. The drawback of this method is that there is no guarantee of achieving the optimal level of satisfaction. For this purpose, the RFPM is represented as follows.

$$\text{Min } f(x) = I_{xx} + I_{yy} + I_{zz} + \gamma \times \left[ sM_i + \left( \frac{(sO - sM) - (sM - sP)}{3} \right) \right] \times (1 - \alpha) \quad (56)$$

s.t.

$$fr_i \geq r_i - \left( sM_i + \left( \frac{(sO - sM) - (sM - sP)}{3} \right) \right) \times (1 - \alpha_i) \quad i \in \text{cubic equipments} \quad (57)$$

$$fr_i \geq r_i \quad i \in \text{cylinder equipments} \quad (58)$$

$$(fr_i + fr_{i+1})^2 \leq (x_i - x_{i+1})^2 + (y_i - y_{i+1})^2 \quad i \in \text{cubic equipments} \quad (59)$$

$$0 \leq \alpha \leq 1. \quad I_{xx}, I_{yy}, I_{zz}, fr \geq 0 \quad (60)$$

In this model, in addition to minimizing moments of inertia, a new section has been added to the objective function, which depicts the total cost of the penalty for possible non-compliance with the flexible constraints. In essence, this phase controls the feasibility and robustness of flexible constraints.

In other words, this expression shows the difference between the minimum and maximum possible values for the flexible constraint, as follows:

$$\begin{aligned} & \left( sM_i + \left( \frac{(sO - sM) - (sM - sP)}{3} \right) \right) \times (1 - \alpha_i) \\ &= r_i - \left[ r_i - \left( sM_i + \left( \frac{(sO - sM) - (sM - sP)}{3} \right) \right) \times (1 - \alpha_i) \right] \end{aligned} \quad (61)$$

$i \in \text{cubic equipments}$

In this model, the penalty cost for each unit of violation of the soft constraint is also considered, as is represented by the parameter  $\gamma$ . In the RFPM, unlike the initial flexible programming model, the minimum level of satisfaction ( $\alpha$ ) is no longer a parameter and is determined by the model as a variable.

Therefore, when solving the model at once, the optimal value of this variable can be achieved, and there is no need to repeat the experiments. Because the objective function of the model seeks a balance between the robustness cost (the last expression of the objective function) and the overall performance of the system, including other expressions of the objective function (such as moments of inertia), the proposed model is called a realistic RFPM.

It should be noted that the parameter  $\gamma$  is an important value, and its value is determined based on the application and the subject under discussion. Here, for example, for cuboid components that need to be placed at a greater distance from other equipment, the value of the penalty parameter can be set as much greater; in this case, the variable  $\alpha$  will

tend to increase to near 1, and therefore the soft constraint for this piece of equipment will become similar to those of cylindrical components.

It should be noted that the use of the penalty parameter in the objective function helps to optimize the variable of minimum satisfaction level ( $\alpha$ ), and prevents the direct involvement of decision-makers in quantifying this variable.

### 3. Results and Discussion

In this section, the efficiency of the proposed model is investigated by comparing its performance with those of previous models in a review of the literature.

Since some of the constraints of the model are flexible, new parameters are introduced that are valued for their possible ability to exceed the aforementioned constraints. For this purpose, the maximum permissible flexibility for soft constraints (sT) is considered.

To analyze the sensitivity of a model based on flexible robust planning, we must first compare it with a simple flexible model with certain levels of satisfaction (for example,  $\alpha = 0.0, 0.1, 0.2, 0.3$ ). The numerical examples used in [1,12,15] were used for this purpose. These three numerical examples have served as the foundation for numerous papers; therefore, the results shown in the eleven articles that used these numerical examples are compared to the results of the suggested model. The multi-layer satellites investigated in the following case studies have a similar structure and layout to those of the geostationary communications satellites of the INTELSAT III series that were designed, assembled, and finally launched successfully several times between 1968 and 1970. The use of new optimization methods and algorithms can reduce the time required for satellite layout design and the related steps, and can help in improving the mass properties as well as the stability and controllability parameters of real satellite projects.

#### - Case Study 1: Investigating the work of [12]

In this example, there are 53 pieces of equipment, of which 24 are cuboids and 29 are cylindrical. In this example, the satellite equipment is arranged across two levels and four layers. As shown in Figure 2, the parameters of the satellite body are as follows: the radius of the circular cross-section of the satellite surface is 500 mm; the radius of the middle cylinder in the satellite connecting the surfaces is 100 mm; the  $H_1$ ,  $H_2$  and  $H_t$  parameters are 300 mm, 830 mm and 1150 mm, respectively, and the diameters of the first and second levels are 20 mm each. The empty satellite consists of four plates (two middle levels and two floor and top levels of the satellite), and the satellite shell and its middle cylinder weigh 776.53 kg. To perform more accurate calculations, it was assumed that the density of materials used in the body of this satellite was  $3.006 \text{ g/cm}^3$  (a combination of aluminum and titanium alloys), and the thickness of the satellite's shell was 41.25 mm. Also, the two middle plates on which components are placed were considered to be hollow cylinders with inner and outer diameters of 100 and 500 mm, respectively, and the upper and lower plates were considered as complete cylinders with 100 mm diameters. According to these hypotheses, it was simple to calculate the weights of each component in the satellite, and to determine the satellite's moment of inertia (as  $I_{x0} = I_{y0} = 185.24$  and  $I_{z0} = 155.2 \text{ kg.m}^2$ ). Since the moment of inertia is higher with an empty satellite than when the components are added, it is expected that the values for the moment of inertia in each of the principal directions of the coordinate axes will be greater than the values calculated for an empty satellite compartment. Also, the coordinates of the center of gravity of the empty satellite were calculated as  $C_0 = (0, 0, 595)$ .

This case was first introduced by [12,16], after which [25,28] also used the data of this numerical example, and compared their results with each other. Ref. [16] similarly utilized comparable data, but the coordinates of their resulting layout were not given for comparison with other studies. With the assumptions mentioned above and according to the coordinates of the equipment after placement in the mentioned articles, the moments of inertia were recalculated and the results were compared, which can be seen in Table 2.

**Table 2.** Comparison of moments of inertia of articles with similar data.

References	Moment of Inertia			
	$I_{xx}$ (kg.m <sup>2</sup> )	$I_{yy}$ (kg.m <sup>2</sup> )	$I_{zz}$ (kg.m <sup>2</sup> )	$f$ (kg.m <sup>2</sup> )
[12]	261	268.5	225.8	755.3
[16]	268.4	271.1	232.7	772.2
[25]—Ex. 2	264.4	261.5	222.2	748.1
[28]	270	265.7	231.9	767.7

As illustrated in Table 2, the best solution in all these articles was given by [25], wherein the achieved objective function was less than the others. Therefore, in this paper, we have used the output in this paper to determine the  $\theta_i$  of cuboid equipment.

Then, using the heuristic method provided in Section 2.1.1, all conceivable modes of allocation of equipment to different layers with these data were investigated, and 25 viable models of equipment allocation were determined. Here, each of these models were implemented using the RFPM described in Section 2.1.2 and GAMS software, and the results have been compared to those of previous works that utilized these data (Table 3).

**Table 3.** Moments of inertia for feasible states in case study 1.

No.	$I_{xx}$ (kg.m <sup>2</sup> )	$I_{yy}$ (kg.m <sup>2</sup> )	$I_{zz}$ (kg.m <sup>2</sup> )	$f$ (kg.m <sup>2</sup> )	No.	$I_{xx}$ (kg.m <sup>2</sup> )	$I_{yy}$ (kg.m <sup>2</sup> )	$I_{zz}$ (kg.m <sup>2</sup> )	$f$ (kg.m <sup>2</sup> )
1	256.3	254.5	220.1	730.8	14	255	256.4	220.3	731.8
2	257.6	257.2	232.9	747.6	15	254.2	257.6	220.4	732.2
3	252.9	254.1	224.5	731.5	16	256.2	255.1	219.3	730.6
4	255.5	257.9	224.1	737.5	17	256.3	255.7	219.7	731.7
5	254.7	257.9	226.9	739.6	18	257.3	256.3	220.9	734.5
6	253.9	256.5	224.2	734.6	19	256.5	258.7	222.1	737.4
7	254.5	254.9	220.9	730.3	20	256.4	257.4	224.7	738.5
8	255.7	253.7	220.3	729.6	21	256.9	257.6	220.3	734.8
9	255.1	253.8	219.2	728.1	22	256.1	257.8	219.1	733
10	255.2	255.9	221.2	732.3	23	259.6	261.1	225.4	746.2
11	256.5	259.7	226.2	742.4	24	259.5	256.2	219.6	735.3
12	260.8	255.1	227.6	743.5	25	261	262.5	226.9	750.4
13	255.3	255.9	220.4	731.6					

As can be seen from the table, the minimum moment of inertia is associated with possible state number 9, in which the total moment of inertia in the main directions of the coordinate axes is equal to 728.1 kg.m<sup>2</sup>, and on the other hand, in 24 of the 25 possible states, the total moment of inertia is slightly better than that given by [25]. Figures 4 and 5 and Table 4 depict the outputs of the model for a case wherein the sum of the moment of inertia is at its lowest possible value (layout of equipment on different layers of the satellite) and the coordinates of the equipment in this optimal state, respectively. In Figure 4, a total number of 29 cylindrical and 24 cubic components are finally placed in optimal locations on the four layers (i.e.,  $L_1, L_2, L_3, L_4$ ) or two middle plates of a satellite with a general cylindrical configuration. Figure 5 also shows the numbers and locations of cylindrical and cubic parts allocated to the four layers of the satellite based on the optimal layout.

To compare the best solutions obtained (Table 3) with a flexible model in the flexible state, we have run the model in all possible modes and compared the objective functions with each other. The results can be seen in Figure 6.

As demonstrated in Figure 6, in cases where the minimum level of satisfaction required to exceed the flexible constraints ( $\alpha$ ) is greater than 0.4, the models will not be responsive in the flexible state, because, if this parameter tends to 1, the constraint loses its flexibility,

and the rectangular radius of the cuboid equipment becomes equivalent to the radius of its circumference, and the limit of no overlap between the pieces of equipment will not be met.

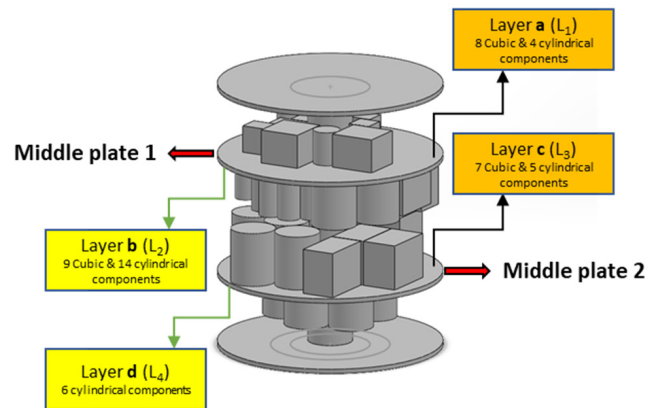


**Figure 4.** Layout of equipment (i.e., placement of a total of 29 cylindrical and 24 cubic components with different sizes and masses) on different layers (i.e.,  $L_1, L_2, L_3, L_4$ ) of the satellite in the optimal state.

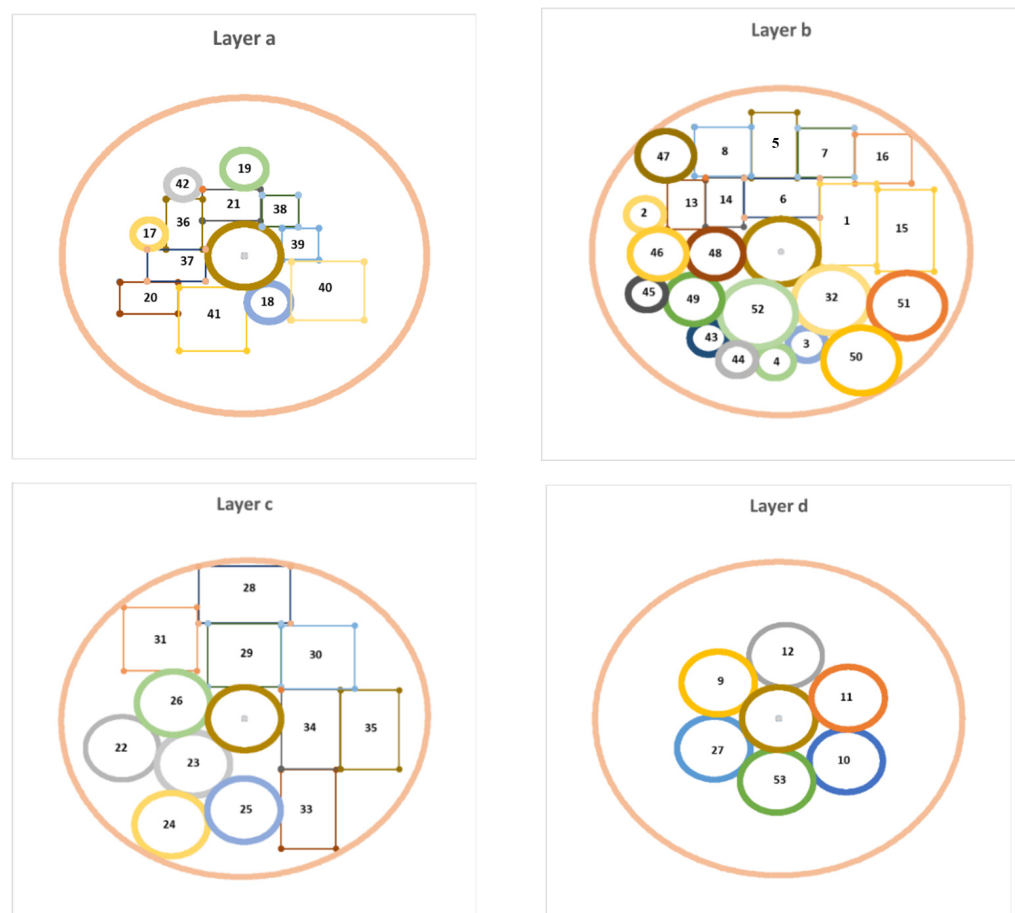


**Figure 5.** Top view of the optimal allocation and layout of equipment on different layers (layer (a) ( $L_1$ ), layer (b) ( $L_2$ ), layer (c) ( $L_3$ ) and layer (d) ( $L_4$ )) of the cylindrical satellite.

Table 4. Optimal dimensions and coordinates of equipment in case study no. 1.

No	Dimensions (mm)			Mass (kg) mi	Optimal Coordinates		Θi (rad)	Layer	No	Dimensions (mm)		Mass (kg) mi	Optimal Coordinates		Layer
	ai/ri	bi	hi		xi (mm)	yi (mm)				ri	hi		xi (mm)	yi (mm)	
1	150	250	200	22.50	329.47	64.86	$\pi/2$	$L_2$	28	100	240	26.62	-1.58	-288.80	$L_3$
2	150	250	200	22.50	177.47	82.86	$\pi/2$	$L_2$	29	100	240	26.62	-193.90	49.01	$L_3$
3	150	250	200	22.50	174.13	-285.90	$\pi/2$	$L_3$	30	100	180	16.97	-175.93	-95.12	$L_4$
4	160	250	200	24.00	180.21	-33.62	$\pi/2$	$L_3$	31	100	180	16.97	189.11	65.10	$L_4$
5	160	250	200	24.00	341.89	-35.46	$\pi/2$	$L_3$	32	100	180	16.97	19.82	199.02	$L_4$
6	250	180	200	27.00	0.07	391.00		$L_3$	33	100	180	16.97	-164.75	113.40	$L_4$
7	200	200	250	30.00	-0.30	200.34		$L_3$	34	100	180	16.97	183.52	-134.83	$L_4$
8	200	200	250	30.00	200.37	193.88		$L_3$	35	100	200	18.85	211.87	-332.71	$L_2$
9	200	200	250	30.00	-229.55	251.01	$\pi/2$	$L_3$	36	100	200	18.85	333.30	-164.84	$L_2$
10	150	150	250	16.88	118.90	302.23	$\pi/2$	$L_2$	37	100	200	18.85	-61.62	-190.27	$L_2$
11	150	150	250	16.88	-153.95	305.58	$\pi/2$	$L_2$	38	100	200	18.85	133.97	-148.50	$L_2$
12	150	150	250	16.88	270.27	283.38		$L_2$	39	75	200	10.60	-324.88	-7.36	$L_2$
13	100	150	200	9.00	-250.46	143.29	$\pi/2$	$L_2$	40	75	200	10.60	-304.87	293.12	$L_2$
14	100	150	200	9.00	-149.32	150.71	$\pi/2$	$L_2$	41	75	200	10.60	-174.88	-6.50	$L_2$
15	100	100	150	4.50	98.32	140.94		$L_1$	42	75	200	10.60	-230.85	-145.67	$L_2$
16	100	100	150	4.50	153.65	36.60		$L_1$	43	50	200	4.71	-359.25	112.82	$L_2$
17	200	185	150	16.65	228.81	-111.59		$L_1$	44	50	200	4.71	67.92	-283.18	$L_2$
18	185	200	150	16.65	-86.89	-200.66	$\pi/2$	$L_1$	45	50	200	4.71	-16.60	-336.62	$L_2$
19	200	120	200	14.40	2.14	164.48		$L_2$	46	50	200	4.71	-191.98	-264.47	$L_2$
20	120	200	200	14.40	-18.22	325.14	$\pi/2$	$L_2$	47	50	200	4.71	-116.38	-329.92	$L_2$
21	160	100	120	1.92	-261.47	-133.58		$L_1$	48	50	200	4.71	-354.70	-128.75	$L_2$
22	160	100	120	1.92	-35.20	159.98		$L_1$	49	60	150	5.09	67.08	-148.29	$L_1$
23	100	160	120	1.92	-165.12	99.19	$\pi/2$	$L_1$	50	60	150	5.09	0.03	273.81	$L_1$
24	160	100	120	1.92	-186.27	-30.91		$L_1$	51	45	160	3.05	-168.36	223.99	$L_1$
25	100		240	26.62	-333.30	-94.41		$L_3$	52	45	160	3.05	-261.07	68.28	$L_1$
26	100		240	26.62	-139.40	-143.42		$L_3$	53	100	180	16.97	-5.59	-199.92	$L_4$
27	100		240	26.62	-200.18	-334.88		$L_3$							

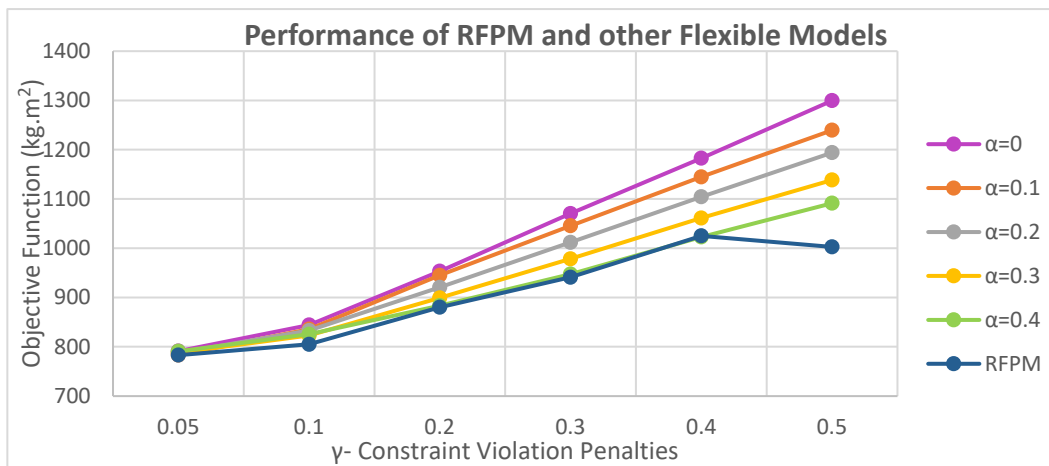


Figure 6. Comparison of the objective function of the RFPM with the flexible models.

It is also clear that when increasing the penalty coefficient for violating the flexible constraints ( $\alpha$ ) in the objective function, the values of the objective function will increase. As a result, the higher the coefficient, the faster the minimum level of satisfaction ( $\alpha$ ) will increase in a flexible model with a lower  $\alpha$ . The reason for this is that, with a decreasing level of satisfaction, the value of  $(1 - \alpha)$  will increase, and the product of the penalty for violating the soft limits by an amount of  $(1 - \alpha)$  in the objective function will increase more sharply.

In the RFPM, the model provides a better solution for all cases; however, when  $\gamma = 0.5$ , this difference will be more pronounced than in other flexible cases, as the penalty coefficients will be increased and the model will attempt to reduce the value of the objective function, causing the minimum value of the satisfaction level ( $\alpha$ ) to increase. Comparing the values of the variables of the minimum satisfaction level ( $\alpha$ ) when  $\gamma = 0.05$  and  $\gamma = 0.5$ , it is obvious that the satisfaction level at  $\gamma = 0.5$  will have a higher value, which, as previously stated, is due to the model’s goal of reducing the objective function, but this can prevent the flexibility of soft constraints increasing, and will increase the value of the moment of inertia by increasing the distances between pieces of equipment.

Therefore, moments of inertia must also be compared to infer the best penalty coefficient.

The total of moments of inertia in the principal directions of the coordinate axes has also been examined using the aforementioned models to determine with which coefficient the model yields the most accurate response. The outcomes are depicted in Figure 7.

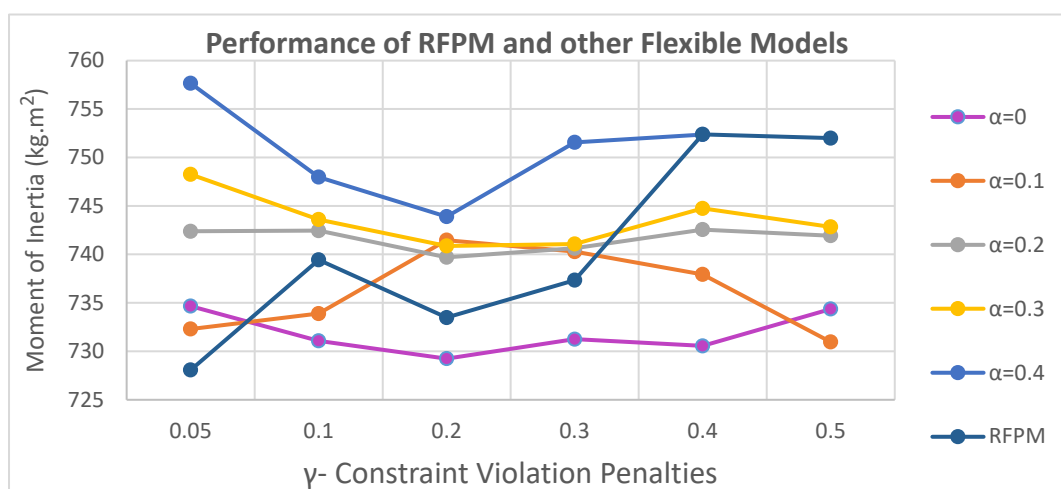
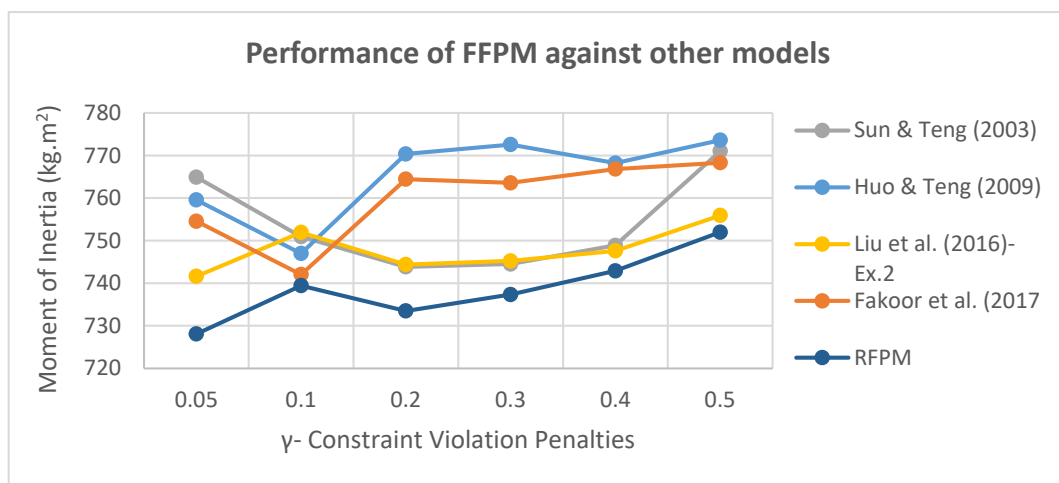


Figure 7. Comparison of the sum of moments of inertia of RFPM produced with flexible models.

As depicted in Figure 7, the greater the minimal satisfaction level ( $\alpha$ ) in flexible models, the greater the amount of the estimated radius of cuboid equipment that will become a circumscribed circle. This model tends to place pieces of equipment further apart from one another, hence increasing the total moments of inertia. An intriguing phenomenon that arises is the distinction between the modifications achieved in the trends under RFPM and flexible models in return for increasing the penalty coefficient for violating soft constraints. This indicates that when increasing the penalty coefficient, the RFPM will produce a greater sum of moments of inertia output. Consequently, the optimal instance for this model is  $\gamma = 0.05$ .

As this coefficient increases, to avoid increasing the objective function of the model, it tries to increase the value of the minimum satisfaction level ( $\alpha$ ), but the RFPM prevents this from occurring, such that the soft constraints are met and the value is not excessively high, causing the objective function to be greater than under flexible states. As a result, the best case for the RFPM is when the value of the penalty coefficient is  $\gamma = 0.05$ . In cases when the cost factor is below this value, the model loses efficiency because the penalty for violating the soft constraints on the objective function is drastically reduced. The model's minimum satisfaction level ( $\alpha$ ) tends towards zero, and the flexible constraints will be in their softest state, which increases the probability of equipment overlapping.

Now that it has been determined that the RFPM is more capable than other flexible models, we will compare this model to the models proposed in prior articles. Here, four articles that used this example in their case studies are analyzed, and the data from each article are used as input for the suggested robust model based on pre-existing equipment positions on different satellite layers. In addition, the model has been applied to these data. The outcomes are depicted in Figure 8.



**Figure 8.** Comparison of the sum of moments of inertia of RFPM with the results of other articles [12,16,25,28].

As shown in Figure 8, the suggested RFPM has a lower total number of moments of inertia than previous articles with all scenarios of penalty coefficients for the violation of soft constraints. Also, the proposed RFPM shows the lowest values of the sum of moments of inertia, at  $\gamma = 0.05$ .

There is a 1.75 percent improvement when comparing the moments of inertia achieved by [25] ( $741.6 \text{ kg.m}^2$ ) and the suggested RFPM ( $728 \text{ kg.m}^2$ ). This implies that if an identical force is required to spin these two satellites, at least 13 kg of mass could be conserved. This improvement will be vital for satellite design specialists seeking to increase the functionality of their products, where every kilogram saved could be essential to a successful mission.

As can be seen, as the penalty coefficient increases, the values of moments of inertia tend to increase due to the objective function seeking to reduce the penalty values, resulting

in less flexibility in soft constraints, as a result of which the pieces of equipment are placed far apart from one another, thereby increasing the total moments of inertia.

- Case Study 2: Investigating the work of [1]

In this example, there are 60 pieces of equipment, of which 24 are cuboids and 36 are cylindrical. In this example, the satellite equipment is arranged across two levels and four layers. The parameters of the satellite body are as follows: the radius of the circular cross-section of the satellite surfaces is 500 mm; the radius of the middle cylinder of the satellite connecting the surfaces is 100 mm; the  $H_1$ ,  $H_2$  and  $H_i$  parameters are 300 mm, 830 mm and 1150 mm, respectively, and the diameters of the first and second levels are 20 mm each.

The empty satellite consists of four plates (two middle levels and two floor and top levels of the satellite), a satellite shell and the middle cylinder, the combined mass of which is 576.53 kg. To perform more accurate calculations, it was assumed that the density of materials used in the body of this satellite was  $3.006 \text{ g/cm}^3$  (a combination of aluminum and titanium alloys) and the thickness of the satellite's shell was 24.5 mm.

Also, the two middle plates on which the components are placed were assumed to be hollow cylinders with inner and outer diameters of 100 and 500 mm, respectively, and the upper and lower plates were assumed to be complete cylinders with 100 mm diameters. Using these hypotheses, the weights of each part of the empty satellite were calculated, and the moment of inertia of the empty satellite was determined to be  $I_{x0} = I_{y0} = 133.24$  and  $I_{z0} = 98.4 \text{ kg.m}^2$ .

Since the moment of inertia is higher for an empty satellite than when the components are added, it is expected that the values obtained regarding the moment of inertia in each of the principal directions of the coordinate axes are greater than these values calculated for an empty satellite. Also, the coordinates of the center of gravity of the empty satellite were calculated as  $C_0 = (0, 0, 595)$ .

Since the case was first introduced by [1], five articles, including those by [17,20,30,36,37] also used the data from this example, and compared their results with each other. Ref. [27] also utilized these numerical data, but the output localizations of the equipment were not organized diagonally, therefore the findings were not comparable. According to the assumptions mentioned above and the coordinates of the equipment placements in the mentioned articles, the moments of inertia have been recalculated and the results compared, as can be seen in Table 5.

**Table 5.** Comparison of moments of inertia in articles with similar data.

References	Moment of Inertia			
	$I_{xx}$ ( $\text{kg.m}^2$ )	$I_{yy}$ ( $\text{kg.m}^2$ )	$I_{zz}$ ( $\text{kg.m}^2$ )	$f$ ( $\text{kg.m}^2$ )
[1]	228.7	232.9	185.1	646.7
[17]	227.8	226	178.2	632
[20]—Ex. 2	228.3	225.8	171.4	625.5
[30]	223.5	220.7	168.4	612.6
[36]	218.2	215.6	166.2	600
[37]—Ex. 3	224.1	228.1	179.7	631.9

As depicted in Table 5, the best solution in these articles was given by [36], where the objective function was less than in other articles. Therefore, in this paper, we have used the output to determine the value of  $\theta_i$  for cuboid equipment. As explained in case study no. 1, here, according to the heuristic method presented in Section 2.1.1, all possible models of equipment allocation to different layers with these data have been examined, and 25 feasible models have been obtained.

Here, each of these feasible models was implemented using the RFPM presented in Section 2.1.2 and GAMS software, and the results have been compared with those from other papers that also used this numerical example (Table 6).

**Table 6.** Moments of inertia for feasible states described in case study 2.

No.	$I_{xx}$ (kg.m <sup>2</sup> )	$I_{yy}$ (kg.m <sup>2</sup> )	$I_{zz}$ (kg.m <sup>2</sup> )	$f$ (kg.m <sup>2</sup> )	No.	$I_{xx}$ (kg.m <sup>2</sup> )	$I_{yy}$ (kg.m <sup>2</sup> )	$I_{zz}$ (kg.m <sup>2</sup> )	$f$ (kg.m <sup>2</sup> )
1	204.8	208.9	164.8	578.5	14	207.9	209.3	171.2	588.5
2	206.8	208.3	164.7	579.8	15	208.3	210.9	169.6	588.8
3	207.7	206.2	166.9	580.8	16	211.3	208.3	169.7	589.3
4	210.8	199.9	170.2	580.9	17	209.1	209.9	172.8	591.8
5	206.6	208.8	167.2	582.4	18	209	212.6	170.6	592.2
6	210.9	207.1	165.8	583.7	19	211.6	210.1	171.2	592.9
7	207.9	207.9	168.2	584	20	209.7	211.3	173.2	594.2
8	209.8	209.2	165.1	584	21	210.8	210.1	174.1	594.9
9	209.8	209.45	166.3	585.5	22	210.9	211.4	173.1	595.5
10	208.2	207.9	169.8	586	23	211.3	211.1	175.3	597.7
11	207.9	208.2	170.8	586.9	24	211.9	208.4	177.7	598.1
12	208.8	208.7	169.6	587.1	25	212.4	211.5	176.5	600.4
13	208.4	207.1	171.5	587.1					

As can be seen in the table, the minimum value of the sum of moments of inertia in the main direction of the coordinate axes is equal to 578.5 kg/m<sup>2</sup>, and in 24 of the feasible states, the sum of moments of inertia derived is slightly better than that given by [36]. Figure 9 and Table 7 show the output of the model for cases where the sum of the moments of inertia is as low as possible (layout of equipment on different layers of the satellite) and the coordinates of the equipment in this optimal model, respectively.

To compare the best solutions obtained (Table 6) with the flexible model in the flexible state, we ran the model in all possible modes and have compared the objective functions with each other. The results can be seen in Figure 10.

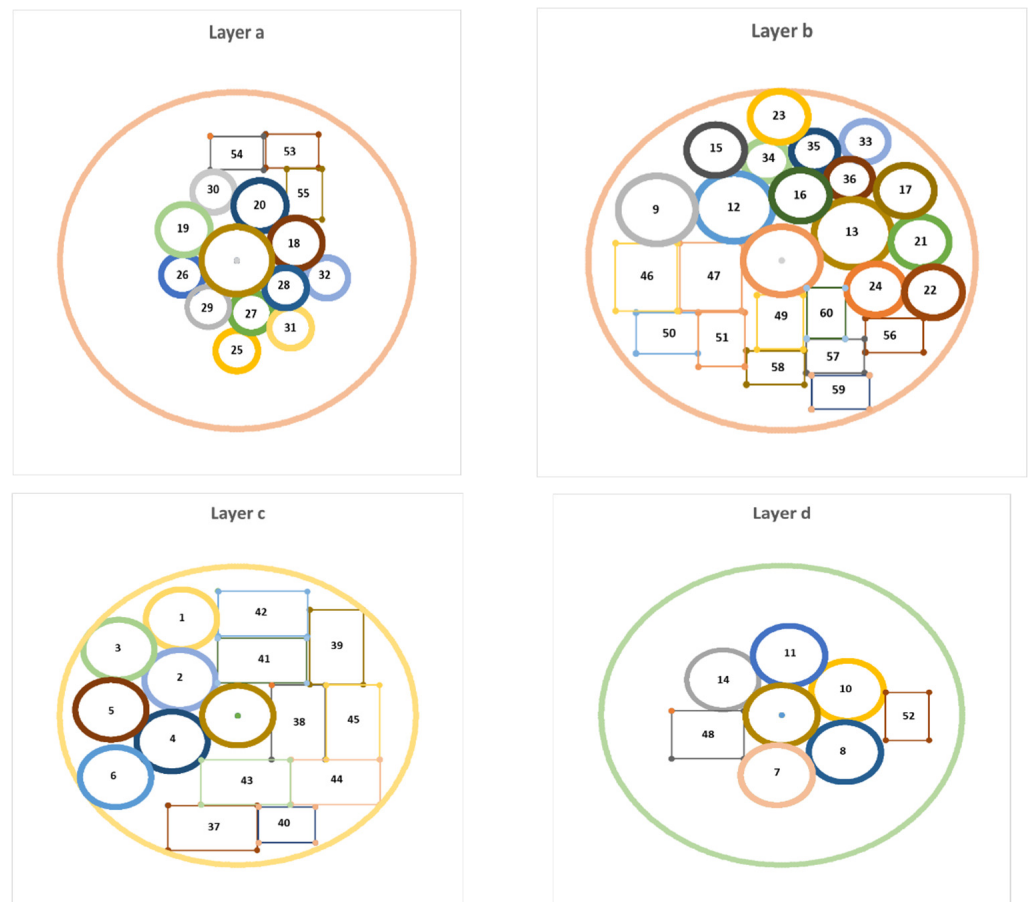
As illustrated in Figure 10, in cases where the minimum level of satisfaction required for exceeding the flexible constraints ( $\alpha$ ) is greater than 0.25, the models will not be responsive in the flexible state because, as in case no. 1, if this parameter tends to 1, the constraint loses its flexibility, and the rectangular radius of the cuboid equipment becomes equivalent to the radius of the circumference, and the constraint of non-overlapping between the equipment will not be met. The only difference from case study no. 1 is that, in flexible states, the minimum level of satisfaction cannot be reached if it is greater than 0.25.

This is due to the increased quantity of equipment to be positioned, which reduces the flexibility of the non-overlap constraints by increasing the ( $\alpha$ ) variable and making the model infeasible. As shown previously, the objective function values increase as the penalty coefficient for violating the flexible constraints ( $\gamma$ ) in the objective function increases. In reality, in flexible models with a smaller ( $\alpha$ ) variable, increasing the value of ( $\gamma$ ) will increase the objective function further. In the RFPM, the model behaves similarly to that in the first case study, and at  $\gamma = 0.5$ , the difference in the output of the objective function between the robust and flexible models becomes more obvious.

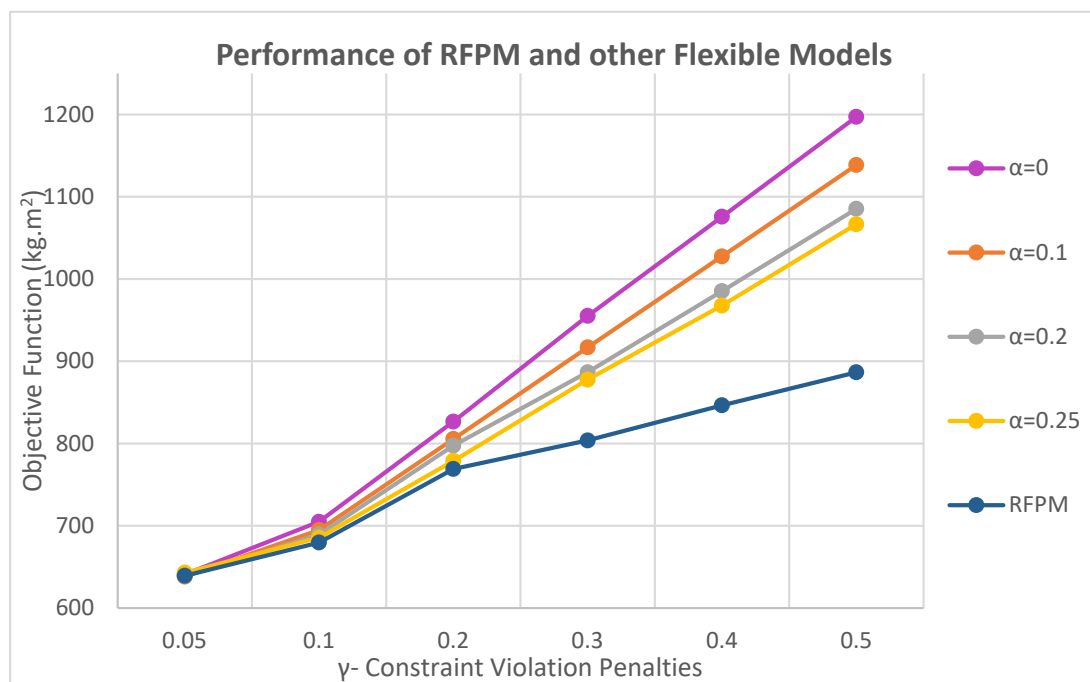
Comparing the values of the variables of the minimum satisfaction level ( $\alpha$ ) for  $\gamma = 0.05$  and  $\gamma = 0.5$ , we see that greater values are obtained for the variable at  $\gamma = 0.5$ , but this leads to an increase in moments of inertia. This implies substantially lower values for ( $\alpha$ ) variables than those seen in case study no. 1 due to the greater quantity of equipment. It indicates that soft constraints must be set to their softest mode to prevent components from overlapping.

Table 7. Optimal dimensions and coordinates of equipment in case study no. 2.

No.	Dimensions (mm)		Mass (kg)	Optimal Coordinates		Layer	No.	Dimensions (mm)			Mass (kg)	Optimal Coordinates		$\theta_i$ (rad)	Layer
	ri	hi		mi	xi (mm)			yi (mm)	ai/ri	bi		hi	mi		
1	100	150	23.56	-157.9	323	L <sub>3</sub>	31	60		150	5.09	152.1	-200.2	L <sub>1</sub>	
2	100	160	23.56	-162.3	119.6	L <sub>3</sub>	32	60		150	5.09	254.4	-51.7	L <sub>1</sub>	
3	100	160	23.56	-334	221	L <sub>3</sub>	33	60		250	5.09	214.8	350.9	L <sub>2</sub>	
4	100	200	23.56	-184.4	-86.5	L <sub>3</sub>	34	60		250	5.09	-39.9	294.2	L <sub>2</sub>	
5	100	200	23.56	-356	19.6	L <sub>3</sub>	35	60		250	5.09	84.6	322.1	L <sub>2</sub>	
6	100	250	23.56	-342.8	-206	L <sub>3</sub>	36	60		250	5.09	174.5	240.1	L <sub>2</sub>	
7	100	120	23.56	-13.6	-200.3	L <sub>4</sub>	37	250	150	150	28.13	-70.6	-376.2	L <sub>3</sub>	
8	100	120	23.56	175.1	-123.6	L <sub>4</sub>	38	250	150	150	28.13	170.3	-22.3	L <sub>3</sub>	
9	100	200	18.85	-323	149.9	L <sub>2</sub>	39	250	150	150	28.13	277.3	229.5	L <sub>3</sub>	
10	100	150	18.85	182.6	81.6	L <sub>4</sub>	40	160	120	250	28.13	138	-365.7	L <sub>3</sub>	
11	100	150	18.85	20.6	198.9	L <sub>4</sub>	41	250	150	250	28.13	68.6	184.1	L <sub>3</sub>	
12	100	160	15.08	-123.2	157.6	L <sub>2</sub>	42	250	150	250	28.13	70.5	341.3	L <sub>3</sub>	
13	100	160	15.08	183.1	80.4	L <sub>2</sub>	43	250	150	250	28.13	22.3	-223.5	L <sub>3</sub>	
14	100	150	15.08	-162	117.3	L <sub>4</sub>	44	250	150	250	28.13	274.5	-222.5	L <sub>3</sub>	
15	75	160	8.48	-171.1	325.9	L <sub>2</sub>	45	250	150	250	28.13	323.45	-22.2	L <sub>3</sub>	
16	75	200	8.48	48.4	192	L <sub>2</sub>	46	200	160	150	19.20	-349.9	-48.2	L <sub>2</sub>	
17	75	250	8.48	318.7	206.3	L <sub>2</sub>	47	200	160	250	19.20	-184	-47.6	L <sub>2</sub>	
18	75	150	8.48	167.3	51.4	L <sub>1</sub>	48	200	160	120	19.20	-204.7	-64.5	L <sub>4</sub>	
19	75	120	7.95	-149.1	91.6	L <sub>1</sub>	49	160	120	250	15.36	-4.2	-181.1	L <sub>2</sub>	
20	75	150	7.95	65.6	162.2	L <sub>1</sub>	50	160	120	250	8.64	-296.7	-213.4	L <sub>2</sub>	
21	75	200	7.95	357	54.7	L <sub>2</sub>	51	160	120	250	8.64	-155.9	-232.2	L <sub>2</sub>	
22	75	250	7.95	391.5	-93.1	L <sub>2</sub>	52	160	120	120	8.64	347.9	-3.8	L <sub>4</sub>	
23	75	250	7.95	-7.2	424.2	L <sub>2</sub>	53	150	100	120	5.40	156.4	324.5	L <sub>1</sub>	
24	75	250	7.95	242	-84.4	L <sub>2</sub>	54	150	100	120	5.40	0.2	319	L <sub>1</sub>	
25	60	150	5.09	0.0	-268.1	L <sub>1</sub>	55	150	100	150	5.40	191.1	197.4	L <sub>1</sub>	
26	60	150	5.09	-154	-43.3	L <sub>1</sub>	56	150	100	160	5.40	290.6	-220.1	L <sub>2</sub>	
27	60	150	5.09	41.1	-154.6	L <sub>1</sub>	57	150	100	160	5.40	138.3	-281.2	L <sub>2</sub>	
28	60	150	5.09	137.9	-80.9	L <sub>1</sub>	58	150	100	200	5.40	-16.4	-315.2	L <sub>2</sub>	
29	60	150	5.09	-79.9	-138.6	L <sub>1</sub>	59	150	100	250	5.40	151.7	-388.2	L <sub>2</sub>	
30	60	150	5.09	-65.9	203.4	L <sub>1</sub>	60	150	100	250	5.40	114.1	-154.6	L <sub>2</sub>	



**Figure 9.** Top view of the optimal allocation and layout of equipment on different layers (layer (a) ( $L_1$ ), layer (b) ( $L_2$ ), layer (c) ( $L_3$ ) and layer (d) ( $L_4$ )) of the cylindrical satellite.



**Figure 10.** Comparison of the objective function of the RFPM with flexible models.

Therefore, the sum of moments of inertia in the main directions of the coordinate axes has also been compared for the mentioned models, and the results can be seen in Figure 11.

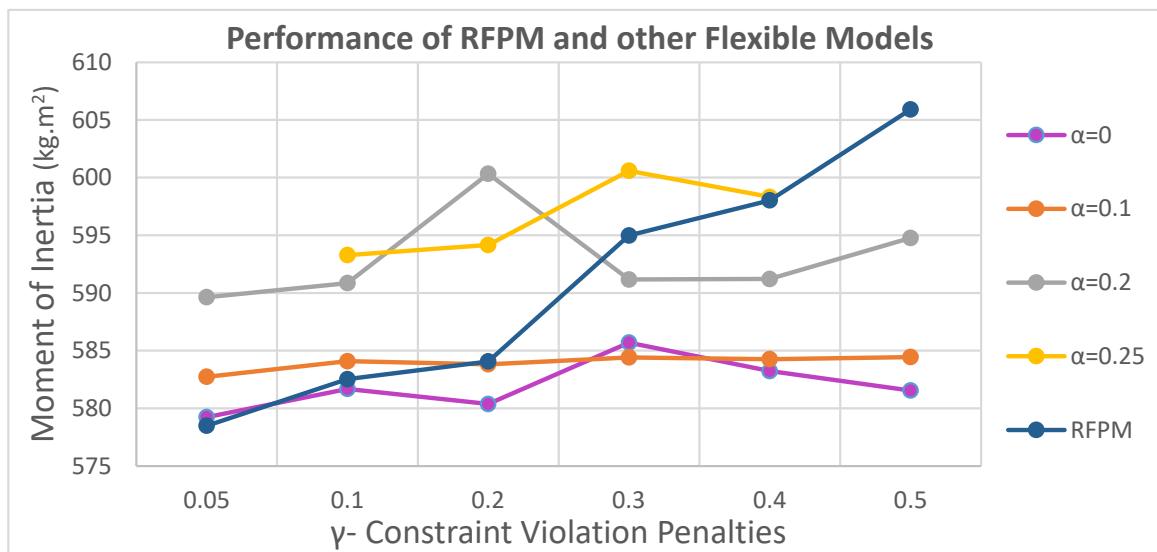


Figure 11. Comparison of the sum of moments of inertia of RFPM with those of flexible models.

As depicted in Figure 11, the behavior of the models has not changed significantly from those in case study no. 1, and it is only due to the increase in the number of equipment that the flexibility of soft constraints becomes more important; even for the flexible models where the minimum satisfaction level ( $\alpha$ ) exceeds 0.25, the model is infeasible. Similarly, when increasing the penalty factor ( $\gamma$ ), the model in its robust form will gain more moments of inertia, due to the tendency of the model to shrink the objective function and increase the  $\alpha$  variables, as well as the tendency of the equipment to move away from one another and raise the moments of inertia.

As a result, the best case for the RFPM is when  $\gamma = 0.05$ . As said before, in cases when the value of the cost factor is lower than this, the model loses its efficiency because the penalty for violating the soft constraints in the objective function is sharply reduced; the minimum level of satisfaction ( $\alpha$ ) of the model tends towards zero, and this causes the flexible constraints to enter their softest mode, increasing the likelihood of the equipment overlapping.

Now that it has been seen that the RFPM has greater capability compared to the other flexible models, we now compare this model with those proposed in similar articles. Here, five articles that used this example in their case studies have been reviewed and, according to the pre-existing equipment layouts on different satellite layers available in the articles, the data of each article have been used as input for the proposed RFPM. The results are shown in Figure 12.

As depicted in Figure 12, the sum of moments of inertia in the suggested RFPM when the penalty coefficients for the violation of soft constraints are less than 0.3 indicates a significantly better solution than in the other articles. Compared to [36], the sum of moments of inertia is increased marginally only in cases when  $\gamma = 0.4$  and  $\gamma = 0.5$ . This confirms that the best choice for the value of the penalty coefficient is  $\gamma = 0.05$ , and that increasing this coefficient reduces the model’s efficiency. Therefore, similar to case study no. 1, an improvement of 2.95 percent can be seen when comparing the moments of inertia between that in [36] (596.1 kg.m<sup>2</sup>) and that achieved by the suggested RFPM (578.5 kg.m<sup>2</sup>). This means that if an identical force is required to spin these two satellites, at least 17.6 kg of mass could be preserved.

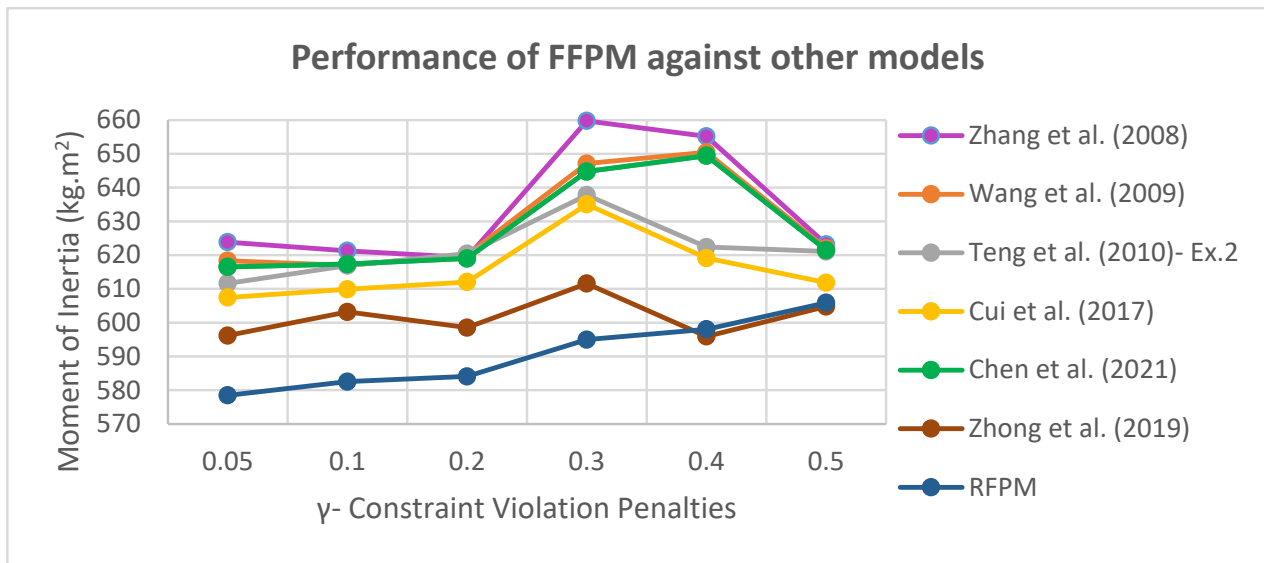


**Figure 12.** Comparison of the sum of moments of inertia of RFPM with the results of other articles [1,17,20,30,36,37].

- Case Study 3: investigating the work of [15]

Ref. [15] utilized the data from [57]. In this example, there are 51 pieces of equipment, of which 20 are cuboid and 31 are cylindrical. In this example, the satellite equipment is arranged across two levels and four layers. The parameters of the satellite body are as follows: the radius of the circular cross-section of the satellite surfaces is 500 mm; the radius of the middle cylinder of the satellite connecting the surfaces is 100 mm; the  $H_1$ ,  $H_2$  and  $H_t$  parameters are 500 mm, 1050 mm and 1400 mm, respectively, and the diameters of the first and second levels are 20 mm each.

The empty satellite consists of four plates (two middle levels and two floor and top levels), the satellite shell and the middle cylinder, the cumulative mass of which is 349.557 kg.

To perform more accurate calculations, it was assumed that the density of materials used in the body of this satellite was  $1.766 \text{ g/cm}^3$  (a combination of fiberglass, Kevlar, carbon fiber, and aluminum and titanium alloys) and the thickness of the satellite shell was 20 mm. Also, the two middle plates on which equipment are placed were considered to be hollow cylinders with inner and outer diameters of 100 and 500 mm, respectively, and the upper and lower plates were considered to be complete cylinders with a 100 mm diameter. According to these hypotheses, the weight of each part of the empty chamber of the satellite was calculated, and the moment of inertia of the empty satellite was calculated, as  $I_{x0} = I_{y0} = 101.556$  and  $I_{z0} = 56.686 \text{ kg.m}^2$ .

Since the moment of inertia is higher for the empty satellite than when the equipment is added, it is expected that the values obtained for the moments of inertia in each of the principal directions of the coordinate axes will be greater than the values calculated for an empty satellite compartment. The coordinates of the center of gravity of the empty satellite were calculated as  $C_0 = (0, 0, 732.96)$ .

After [15], the first study to utilize these numerical data and compare their results was [25]. Ref. [13] also employed similar data, but the coordinates of their output design were not disclosed in that article to allow comparisons with other studies. According to the assumptions mentioned above and the coordinates of the placed equipment available in the mentioned articles, the moments of inertia have been recalculated and the results compared, as can be seen in Table 8.

**Table 8.** Comparison of moments of inertia of articles with similar data.

References	Moment of Inertia			
	$I_{xx}$ (kg.m <sup>2</sup> )	$I_{yy}$ (kg.m <sup>2</sup> )	$I_{zz}$ (kg.m <sup>2</sup> )	$f$ (kg.m <sup>2</sup> )
[15]	174.5	171.3	101	446.8
[25]—Ex. 1	163.2	162.9	93.8	420

As can be seen in Table 8, the best solution given by these two articles was produced by [25], in which the objective function was given a lower value compared to other articles. Therefore, in this paper, we have used the output to determine the  $\theta_i$  value for cuboid equipment. Then, according to the heuristic method presented in Section 2.1.1, all possible models of equipment allocation to different layers using these data have been examined, and 11 feasible models have been obtained. Here, each of these models was implemented using the RFPM presented in Section 2.1.2 and GAMS software, and the results have been compared with those from other papers that used this dataset (Table 9).

**Table 9.** Moments of inertia for feasible states in case study 3.

No.	$I_{xx}$ (kg.m <sup>2</sup> )	$I_{yy}$ (kg.m <sup>2</sup> )	$I_{zz}$ (kg.m <sup>2</sup> )	$f$ (kg.m <sup>2</sup> )	No.	$I_{xx}$ (kg.m <sup>2</sup> )	$I_{yy}$ (kg.m <sup>2</sup> )	$I_{zz}$ (kg.m <sup>2</sup> )	$f$ (kg.m <sup>2</sup> )
1	147.7	149.5	100.7	397.9	7	149.9	150.9	96.8	397.6
2	149.2	150.7	95.7	395.6	8	148.5	149.7	98.9	397.1
3	149.4	150.7	99.8	399.9	9	149.9	150.2	97.6	397.7
4	148.5	150.4	99.6	398.5	10	149.2	150.9	98.5	398.5
5	148.6	150	101.2	399.8	11	153.6	152.1	102.7	408.4
6	149.1	149.4	100.6	399.1					

As can be seen from the table, the minimum moment of inertia correlates with the second possible state, in which the total moment of inertia in the main direction of the coordinate axes is equal to 395.6 kg.m<sup>2</sup>, and on the other hand, in all possible states, the total moment of inertia derived is better than that achieved by [25]. Figure 13 and Table 10 show the output of the model when the value of the sum of the moments of inertia is as low as possible (layout of equipment on different layers of the satellite) and the coordinates of the equipment in this optimal state, respectively.

To compare the best solutions obtained (Table 9) with those given by the flexible model in the flexible state, we have run the model in all possible modes and compared the objective functions with each other. The results can be seen in Figure 14.

As shown in Figure 14, in cases where the minimum level of satisfaction for exceeding the flexible constraints ( $\alpha$ ) is greater than 0.3, the models will not be responsive under the flexible state because, as we saw in case studies 1 and 2, by increasing the value of ( $\alpha$ ), flexibility is lost, and the rectangular radius of the cuboid equipment becomes equivalent to the radius of the circumference. As a result, the requirement of non-overlap between the pieces of equipment will not be met.

The only difference from previous case studies is that, in flexible states, the minimum level of satisfaction becomes inapplicable if it increases from 0.3. The reason is that the equipment here occupies more space than in case study no. 1, but less compared to case study no. 2, and therefore setting  $\alpha = 0.3$  also offers a feasible model. As said before, by increasing the penalty coefficient for a violation of the flexible constraints ( $\gamma$ ) in the objective function, the objective will be increased, as the number of flexible models with a lower minimum degree of satisfaction ( $\alpha$ ) will increase dramatically as this coefficient increases.



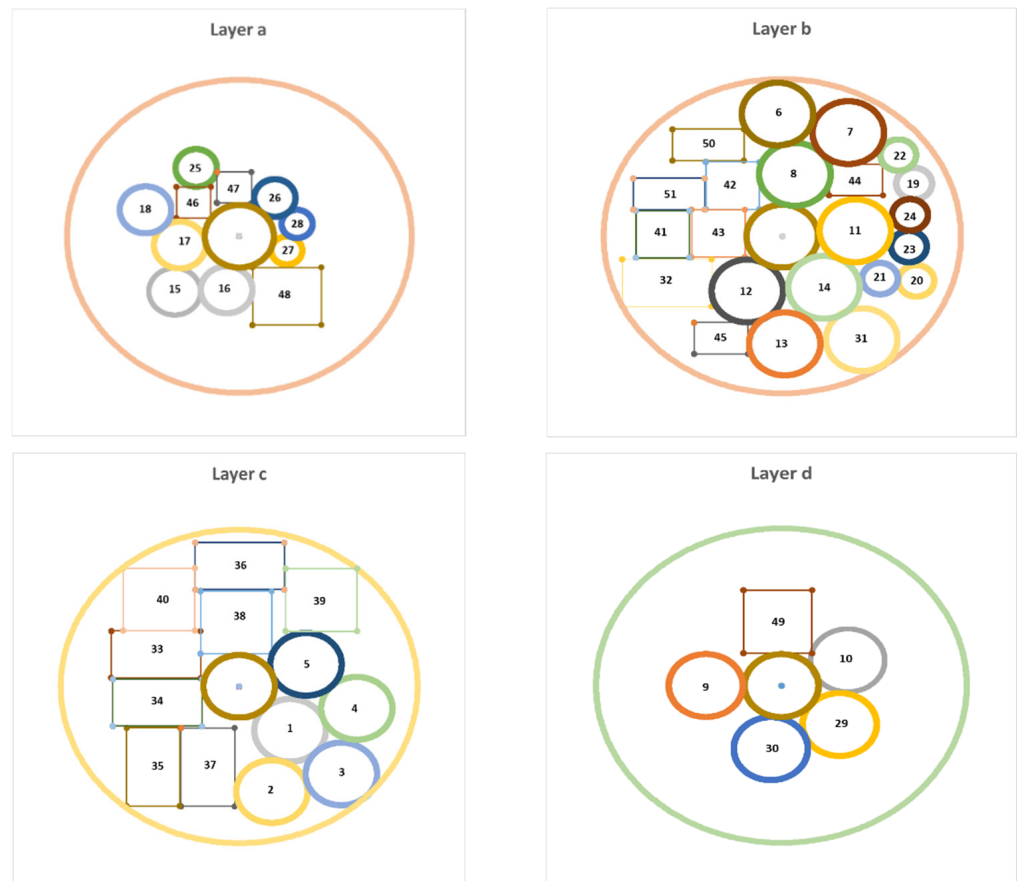


**Figure 13.** Top view of the optimal allocation and layout of equipment on different layers (layer (a) ( $L_1$ ), layer (b) ( $L_2$ ), layer (c) ( $L_3$ ) and layer (d) ( $L_4$ )) of the cylindrical satellite.

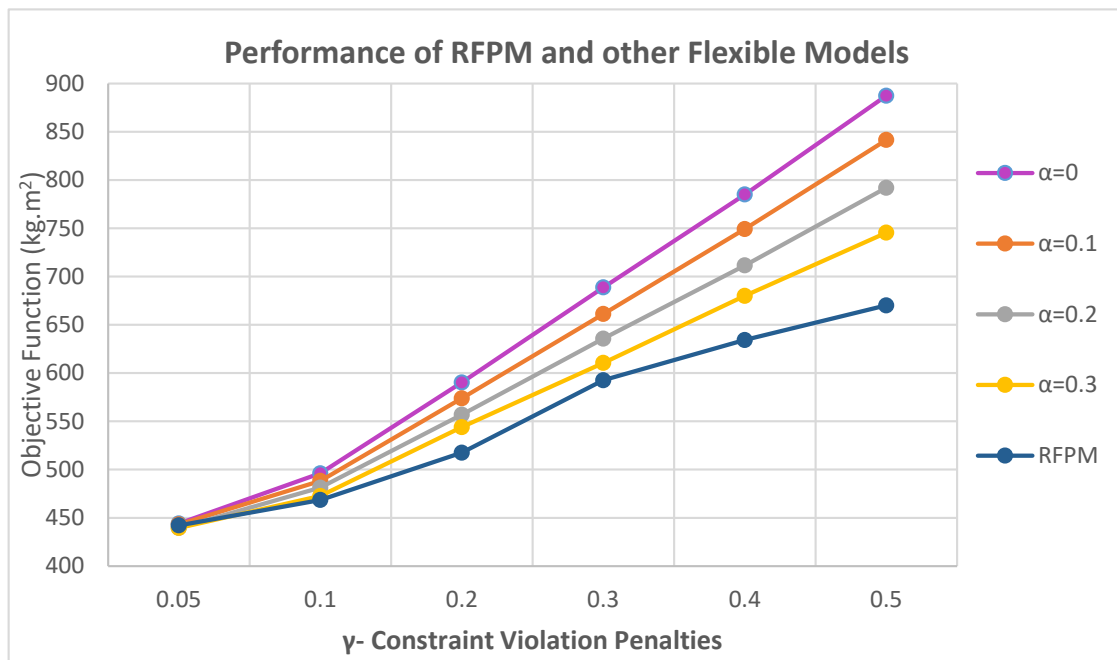


**Figure 14.** Comparison of the objective function of the RFPM with those of the flexible models.

In the robust state, the model acts similarly to in the previous case studies, and at  $\gamma = 0.5$ , the difference in the objective function for flexible models will be more obvious.

When comparing the minimum satisfaction level variables ( $\alpha$ ) for values of  $\gamma = 0.05$  and  $\gamma = 0.5$ , it is obvious that the values obtained for the  $\alpha$  variable at  $\gamma = 0.05$  are higher than those in previous case studies, and it is only the location of the equipment that allows the robust model to limit the flexibility of soft constraints by increasing the values of the minimum satisfaction level ( $\alpha$ ) variables. As a result, these non-overlap constraints are met more easily (lower penalty in the objective function).

To offer a more detailed study, the sums of the moments of inertia in the main directions of the coordinate axes were also compared for the mentioned models, and the results can be seen in Figure 15.

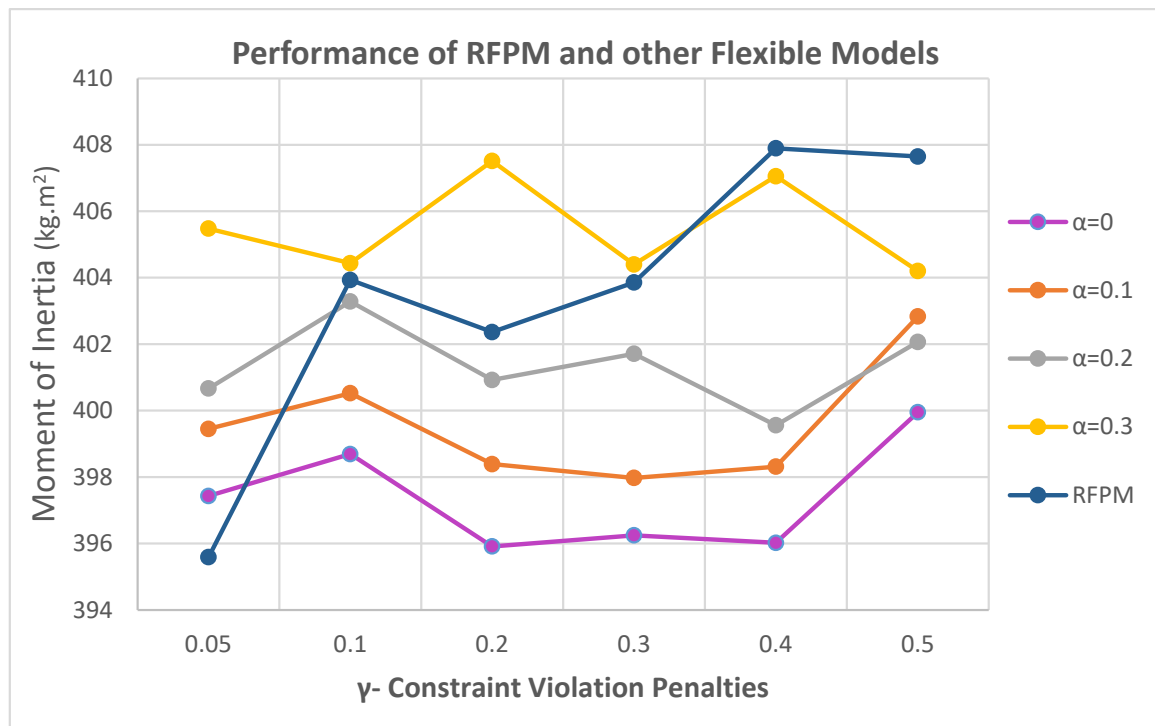
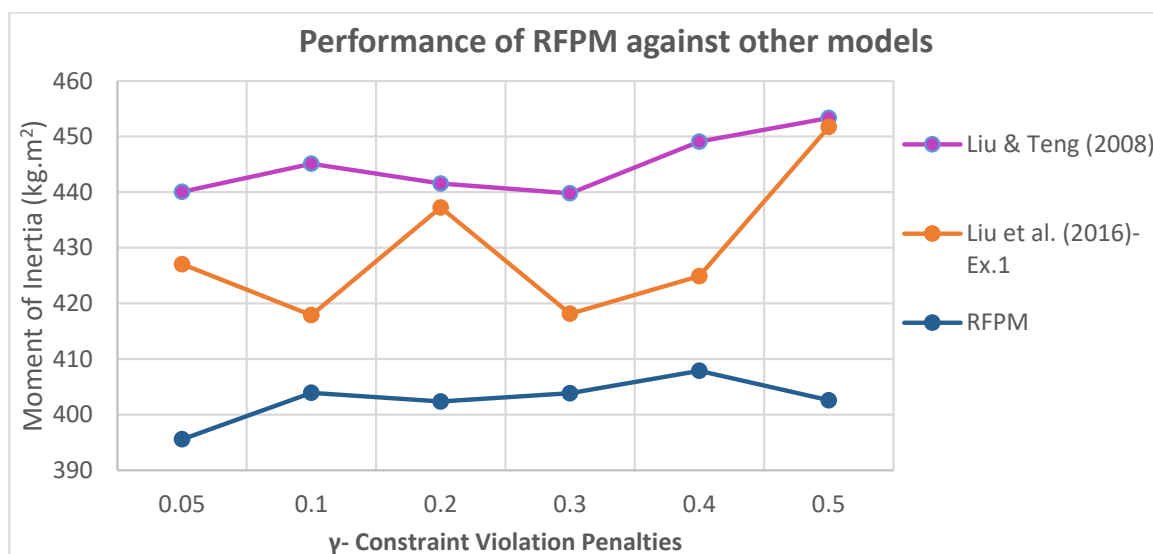


Figure 15. Comparison of the sums of moments of inertia of RFPM with those of flexible models.

As can be seen in Figure 15, in general, the behaviors of the models are not very different compared to those in previous case studies, and by increasing the penalty coefficient  $\gamma$ , the model can be made to gain more moments of inertia in the robust state, due to the same tendency of the model to reduce the objective function by increasing the  $\alpha$  variables. This will result in the pieces of equipment being placed far apart from one another, thereby increasing the total moments of inertia.

Therefore, as in case studies 1 and 2, the best case for an RFPM is when  $\gamma = 0.05$ . As before, in cases with a cost factor below this value, the model loses its efficiency because the penalty for violating the soft constraints in the objective function is sharply reduced, and the model's minimum level of satisfaction ( $\alpha$ ) tends towards zero and leads to the flexible constraints adopting their softest state, increasing the probability of equipment overlap. As before, we now compare the robust model presented here with the models proposed in similar articles.

Here, two articles that used this example in their case studies have been examined, and, according to the pre-existing equipment layout designs for different satellite layers that are available in the articles, the data from each article have been used as the input for the proposed robust model. The results are illustrated in Figure 16.



**Figure 16.** Comparison of the sum of moments of inertia of RFPM with the results of other articles [15,25].

As can be seen in Figure 16, the sum of moments of inertia for the proposed RFPM in all cases of penalty coefficients for the violation of soft constraints is much lower than in other articles. Also, as in previous case studies, the best and lowest values for the sum of moments of inertia can be seen in the proposed RFPM when  $\gamma = 0.05$ .

Similar to other case studies, an improvement of 7.35 percent may be seen when comparing the moments of inertia between [25] (427 kg.m<sup>2</sup>) and the suggested RFPM (395.6 kg.m<sup>2</sup>). This suggests that if an identical force is required to spin these two satellites, at least 31.4 kg of mass can be preserved.

Finally, when increasing the penalty coefficient, the values of moments of inertia tend to increase due to the objective function trying to reduce the penalty values. As a result, the soft constraints will be less flexible, as a result of which the equipment will be placed at great distances, thereby increasing the total moments of inertia.

#### 4. Conclusions

In this study, the optimal allocation and layout of equipment in a three-dimensional satellite space are investigated. Stratified satellites were here discussed, and to measure performance, research was conducted on satellite containers with the most floors. According to the literature, the majority of satellite categories have two levels and four layers, with a total of eleven case studies discussed here using these numbers of levels and layers. In this study, the performance of the suggested model was assessed by comparison with all of the examples from these 11 publications, which were analyzed in three separate cases.

In every instance, it was demonstrated that the flexible model delivers a far superior solution compared to the models presented in prior articles.

In other words, developing an optimum solution for allocating and locating equipment using an optimization method instead of trial-and-error is the contribution of this article.

Although some authors have considered constraints related to thermal distributions, such as [23,26], no studies have taken into account the importance of the distance between components with greater thermal energy. Therefore, components that produce and emit more thermal energy must be as far away from each other as possible. For instance, to ensure better performance and a longer battery life, these components should be kept away from equipment that generates greater heat. In this case, using the concept of the obnoxious facility location problem (reviewed by Zanjirani Farahani and Hekmatfar (2009) [58]) would be appropriate when locating the best positions of these components within the satellite. The concept of uncertainty can be applied here. For problematic equipment, the required distance values are unknown in advance. Possibilistic programming is useful when there

is “uncertainty in the data”. As a consequence, it would be feasible to model some of these problems using flexible programming under uncertainty, and some using possible programming, when it comes to problematic equipment.

Since one of the sources of uncertainty is measurement errors, and the issue of tolerance design plays a significant role in the conceptual design phase of the layout of satellite equipment, the issue of uncertainty when determining the distances between components is another appropriate use of the uncertainty concept, and this can enhance the performance of the model by satisfying the functional and equilibrium constraints, which will ultimately lead to model optimization.

Another topic that could be investigated is the satellite’s temperature field, which would exert a direct influence on the operational performance of electrical components. Generally, a homogeneous distribution of heat flux within the satellite is required to maintain the optimal performance and reliability of its components. Batteries, telemetry senders, and picture senders are examples of components that emit a great deal of energy, and are therefore classified as “hot” components. These components must be positioned at specified distances from each other. Hengeveld et al. (2011a) [59] proposed that their strategy, when paired with another one that they established Hengeveld et al. (2011b) [60], was highly appropriate when distributing individual components with uneven power to different panels of a satellite so as to minimize temperature dispersion within the satellite. From a thermal perspective, each component has an effective area that influences neighboring modules; therefore, decreasing the area of intersection is comparable to increasing the uniformity of the temperature field across the satellite panels. As regards adding thermal constraints, [34] may offer the best reference.

According to all of these interpretations, regarding the calculation of the distances and thermal radii of equipment, soft constraints can be used to calculate the distances of all cuboid and cylindrical pieces of equipment such that they are no closer than a specific limit.

**Author Contributions:** Conceptualization, M.H. and M.R.M.A.; methodology, M.H., M.R.M.A. and T.S.; software, M.H. and M.S.P.; validation, M.H. and M.R.M.A.; formal analysis, M.H., M.S.P. and T.S.; investigation, M.H. and M.S.P.; writing—original draft, M.H. and M.S.P.; writing—review & editing, T.S.; visualization, M.H. and M.S.P.; supervision, M.R.M.A. and T.S.; Project administration, M.R.M.A. All authors have read and agreed to the published version of the manuscript.

**Funding:** T.S. was funded under the grant “Subvention for Science” 492 (MEiN), project No. FD-20/IL-4/046.

**Data Availability Statement:** The data presented in this study are available on request from the corresponding author. The data are not publicly available due to the copyright restrictions.

**Conflicts of Interest:** The authors declare no conflict of interest.

## References

1. Zhang, B.; Teng, H.F.; Shi, Y.J. Layout optimization of satellite module using soft computing techniques. *Appl. Soft Comput.* **2008**, *8*, 507–521. [[CrossRef](#)]
2. Ahmadi, A.; Pishvaei, M.S.; Akbari Jokar, M.R. A survey on multi-floor facility layout problems. *Comput. Ind. Eng.* **2017**, *107*, 158–170. [[CrossRef](#)]
3. Ferebee, M.J., Jr.; Powers, R.B. *Optimization of Payload Mass Placement in a Dual*; Keel Space Station, NASA, Langley Research Centre: Hampton, VA, USA, 1987.
4. Ferebee, M.J.; Allen, C.L. Optimization of payload placement on arbitrary spacecraft. *J. Spacecr. Rocket.* **1991**, *28*, 612–614. [[CrossRef](#)]
5. Rocco, E.M.; Souza, M.; Prado, A. Multi-objective optimization applied to satellite constellations I: Formulation of the smallest loss criterion. In Proceedings of the 54th International Astronautical Congress (IAC’03), Bremen, Germany, 29 September–3 October 2003.
6. Cagan, J.; Shimada, K.; Yin, S. A survey of computational approaches to three-dimensional layout problems. *Comput.-Aided Des.* **2002**, *34*, 597–611. [[CrossRef](#)]
7. Jang, S. A study on three-dimensional layout design by the simulated annealing method. *J. Mech. Sci. Technol.* **2008**, *22*, 2016–2023. [[CrossRef](#)]

8. Zhang, Z.H.; Wang, Y.S.; Teng, H.F.; Shi, Y.J. Parallel Dual-system Cooperative Co-Evolutionary Differential Evolution Algorithm with Human-computer Cooperation for Multi-Cabin Satellite Layout Optimization. *J. Converg. Inf. Technol.* **2013**, *2013*, 711–720.
9. Zhang, Z.H.; Zhong, C.; Xu, Z.Z.; Teng, H.F. A Non-Dominated Sorting Cooperative Co-Evolutionary Differential Evolution Algorithm for Multi-Objective Layout Optimization. *IEEE Access* **2017**, *5*, 14468–14477. [[CrossRef](#)]
10. Zhang, Z.H.; Sun, X.; Hou, L.; Chen, W.; Shi, Y.; Cao, X. A Cooperative Co-Evolutionary Multi-Agent System for Multi-Objective Layout Optimization of Satellite Module. In Proceedings of the 2017 IEEE International Conference on Systems, Man, and Cybernetics (SMC), Banff, AB, Canada, 5–8 October 2017.
11. Teng, H.F.; Sun, S.L.; Liu, D.Q.; Li, Y.Z. Layout optimization for the objects located within a rotating vessel—A three-dimensional packing problem with behavioural constraints. *Comput. Oper. Res.* **2001**, *28*, 521–535. [[CrossRef](#)]
12. Sun, Z.G.; Teng, H.F. Optimal layout design of a satellite module. *Eng. Opt.* **2003**, *35*, 513–529. [[CrossRef](#)]
13. Huo, J.; Shi, Y.; Teng, H.F. Layout design of a satellite module using a human-guided genetic algorithm. In Proceedings of the 2006 International Conference on Computational Intelligence and Security, Guangzhou, China, 3–6 November 2006; pp. 230–235.
14. Chen, W.; Shi, Y.J.; Teng, H.F. An improved differential evolution with local search for constrained layout optimization of satellite module. *Int. Conf. Intell. Comput.* **2008**, 5227, 742–749.
15. Liu, Z.; Teng, H. Human-computer cooperative layout design method and its application. *Comput. Ind. Eng.* **2008**, *55*, 735–757. [[CrossRef](#)]
16. Huo, J.Z.; Teng, H.F. Optimal layout design of a satellite module using a coevolutionary method with heuristic rules. *J. Aerosp. Eng.* **2009**, *22*, 101–111. [[CrossRef](#)]
17. Wang, Y.S.; Teng, H.F.; Shi, Y.J. Cooperative co-evolutionary scatter search for satellite module layout design. *Eng. Comput.* **2009**, *26*, 761–785. [[CrossRef](#)]
18. Huo, J.Z.; Teng, H.F.; Sun, W.; Chen, J. Human-computer co-operative co-evolutionary method and its application to a satellite module layout design problem. *Aeronaut. J.* **2010**, *114*, 209–223. [[CrossRef](#)]
19. Xu, Y.C.; Dong, F.M.; Liu, Y.; Xiao, R.B.; Amos, M. Ant colony algorithm for the weighted item layout optimization problem. *Comput. Sci.* **2010**, *3*, 221–232.
20. Teng, H.F.; Chen, Y.; Zeng, W.; Shi, Y.J.; Hu, Q.H. A dual-system variable-grain cooperative Co-evolutionary algorithm: Satellite-module layout design. *IEEE Trans. Evol. Comput.* **2010**, *14*, 438–455. [[CrossRef](#)]
21. He, K.; Mo, D.; Ye, T.; Huang, W. A coarse-to-fine quasi-physical optimization method for solving the circle packing problem with equilibrium constraints. *Comput. Ind. Eng.* **2013**, *66*, 1049–1060. [[CrossRef](#)]
22. Lau, V.; de Sousa, F.L.; Galski, R.L.; Rocco, E.M.; Becceneri, J.C.; Santos, W.A.; Sandri, S.A. A multidisciplinary design optimization tool for spacecraft equipment layout conception. *J. Aerosp. Technol. Manag.* **2014**, *6*, 431–446. [[CrossRef](#)]
23. Cuco, A.P.C.; Sousa, F.L.D.; Silva Neto, A.J. A multi-objective methodology for spacecraft equipment layouts. *Optim. Eng.* **2015**, *16*, 165–181. [[CrossRef](#)]
24. Fakoor, M.; Taghinezhad, M. Layout and configuration design for a satellite with variable mass using a hybrid optimization method. *Proc. Inst. Mech. Eng. Part G J. Aerosp. Eng.* **2016**, *230*, 360–377. [[CrossRef](#)]
25. Liu, J.; Hao, L.; Li, G.; Xue, Y.; Liu, Z.; Huang, J. Multi-objective layout optimization of a satellite module using the Wang-Landau sampling method with local search. *Front. Technol. Electron. Eng.* **2016**, *17*, 527–542. [[CrossRef](#)]
26. Fakoor, M.; Ghoreishi, S.M.N.; Sabaghzadeh, H. Spacecraft Component Adaptive Layout Environment (SCALE): An efficient optimization tool. *Adv. Space Res.* **2016**, *58*, 1654–1670. [[CrossRef](#)]
27. Li, Z.; Zeng, Y.; Wang, Y.; Wang, L.; Song, B. A hybrid multi-mechanism optimization approach for the payload packing design of a satellite module. *Appl. Soft Comput.* **2016**, *45*, 11–26. [[CrossRef](#)]
28. Fakoor, M.; Mohammad Zadeh, P.; Momeni Eskandari, H. Developing an optimal layout design of a satellite system by considering natural frequency and attitude control constraints. *Aerosp. Sci. Technol.* **2017**, *71*, 172–188. [[CrossRef](#)]
29. Shafae, M.; Mohammadzadeh, P.; Elkaie, A.; Abbasi, S. Layout design optimization of a space propulsion system using a hybrid optimization algorithm. *Proc. Inst. Mech. Eng. Part G J. Aerosp. Eng.* **2017**, *231*, 338–349. [[CrossRef](#)]
30. Cui, F.Z.; Xu, Z.Z.; Wang, X.K.; Zhong, C.Q.; Teng, H.F. A dual-system cooperative co-evolutionary algorithm for satellite equipment layout optimization. *Proc. Inst. Mech. Eng. Part G J. Aerosp. Eng.* **2018**, *232*, 2432–2457. [[CrossRef](#)]
31. Qin, Z.; Liang, Y.G. Layout Optimization of Satellite Cabin Considering Space Debris Impact Risk. *J. Spacecr. Rocket.* **2017**, *54*, 1–5.
32. Xu, Z.Z.; Zhong, C.Q.; Teng, H.F. Assignment and layout integration optimization for simplified satellite re-entry module component layout. *Proc. Inst. Mech. Eng. Part G J. Aerosp. Eng.* **2019**, *233*, 4287–7301. [[CrossRef](#)]
33. Qin, Z.; Liang, Y.; Zhou, J. An optimization tool for satellite equipment layout. *Adv. Space Res.* **2018**, *61*, 223–234. [[CrossRef](#)]
34. Chen, X.; Yao, W.; Zhao, Y.; Chen, X.; Zheng, X. A practical satellite layout optimization design approach based on enhanced finite-circle method. *Struct. Multidiscip. Optim.* **2018**, *58*, 2635–2653. [[CrossRef](#)]
35. Chen, X.; Yao, W.; Zhao, Y.; Chen, X.; Zhang, J.; Luo, Y. The hybrid algorithms are based on differential evolution for satellite layout optimization design. In Proceedings of the 2018 IEEE Congress on Evolutionary Computation (CEC), Rio de Janeiro, Brazil, 8–13 July 2018; IEEE: Piscataway, NJ, USA, 2018; pp. 1–8. [[CrossRef](#)]
36. Zhong, C.Q.; Xu, Z.Z.; Teng, H.F. Multi-module satellite component assignment and layout optimization. *Appl. Soft Comput.* **2019**, *75*, 148–161. [[CrossRef](#)]
37. Chen, X.; Yao, W.; Zhao, Y.; Chen, X.; Liu, W. A novel satellite layout optimization design method based on phi-function. *Acta Astronaut.* **2021**, *180*, 560–574. [[CrossRef](#)]

38. Sun, J.; Chen, X.; Zhang, J.; Yao, W. A niching cross-entropy method for multimodal satellite layout optimization design. *Complex Intell. Syst.* **2021**, *7*, 1971–1989. [[CrossRef](#)]
39. Pühlhofer, T.; Baier, H. Approaches for further rationalisation in mechanical architecture and structural design of satellites. In Proceedings of the 54th International Astronautical Congress of the International Astronautical Federation, the International Academy of Astronautics, and the International Institute of Space Law, Bremen, Germany, 29 September–3 October 2003.
40. Cuco, A. Development of a Multi-Objective Methodology for Layout Optimization of Equipment in Artificial Satellites. Master's Thesis, Postgraduate Course in Space Technology and Engineering, National Institute for Space Research (INPE), Sao Paulo, Brazil, 2011.
41. Pühlhofer, T.; Langer, H.; Baier, H.; Huber, M.B.T. Multi-criteria and Discrete Configuration and Design Optimization with Applications for Satellites. In Proceedings of the 10th AIAA/ISSMO Multidisciplinary Analysis and Optimization Conference, Albany, NY, USA, 30 August–1 September 2004.
42. Albano, A.; Sapuppo, G. Optimal allocation of two-dimensional irregular shapes using heuristic search methods. *IEEE Trans. Syst. Man Cybern.* **1980**, *10*, 242–248. [[CrossRef](#)]
43. Li, Z.; Milenkovic, V. Compaction and separation algorithms for nonconvex polygons and their applications. *Eur. J. Oper. Res.* **1995**, *84*, 539–561. [[CrossRef](#)]
44. Chen, S.; Xuan, M.; Xin, J.; Liu, Y.; Gu, S.; Li, J.; Zhang, L. Design and experiment of dual micro-vibration isolation system for optical satellite flywheel. *Int. J. Mech. Sci.* **2020**, *179*, 105592. [[CrossRef](#)]
45. Chernov, N.; Stoyan, Y.; Romanova, T.; Pankratov, A. Phi-Functions for 2D Objects Formed by Line Segments and Circular Arcs. *Adv. Oper. Res.* **2012**, *2012*, 346358. [[CrossRef](#)]
46. Galbraith, J.R. *Designing Complex Organizations*; Addison-Wesley Longman Publishing Co., Inc.: Reading, MA, USA, 1973.
47. Mula, J.; Poler, R.; Garcia-Sabater, J.P. Material requirement planning with fuzzy constraints and fuzzy coefficients. *Fuzzy Sets Syst.* **2007**, *158*, 783–793. [[CrossRef](#)]
48. Klibi, W.; Martel, A.; Guitouni, A. The design of robust value-creating supply chain networks: A critical review. *Eur. J. Oper. Res.* **2010**, *203*, 283–293. [[CrossRef](#)]
49. Pishvae, M.S.; Fazli Khalaf, M. Novel robust fuzzy mathematical programming methods. *Appl. Math. Model.* **2016**, *40*, 407–418. [[CrossRef](#)]
50. Mulvey, J.; Vanderbei, R.; Zenios, S. Robust optimization of large-scale systems. *Oper. Res.* **1995**, *43*, 264–281. [[CrossRef](#)]
51. Leung, S.C.H.; Tsang, S.O.S.; Ng, W.L.; Wu, Y. A robust optimization model for multi-site production planning problem in an uncertain environment. *Eur. J. Oper. Res.* **2007**, *181*, 224–238. [[CrossRef](#)]
52. Yu, C.S.; Li, H.L. A robust optimization model for stochastic logistic problems. *Int. J. Prod. Econ.* **2000**, *64*, 385–397. [[CrossRef](#)]
53. Ben-Tal, A.; Nemirovski, A. Robust convex optimization. *Math. Oper. Res.* **1998**, *2*, 769–805. [[CrossRef](#)]
54. Ben-Tal, A.; Nemirovski, A. Robust solutions of linear programming problems contaminated with uncertain data. *Math. Program.* **2000**, *88*, 411–424. [[CrossRef](#)]
55. El-Ghaoui, L.; Oustry, F.; Lebret, H. Robust solutions to uncertain semidefinite programs. *SIAM J. Optim.* **1998**, *9*, 33–52. [[CrossRef](#)]
56. Pishvae, M.S.; Razmi, J.; Torabi, S.A. Robust possibilistic programming for socially responsible supply chain network design: A new approach. *Fuzzy Sets Syst.* **2012**, *206*, 1–20. [[CrossRef](#)]
57. Li, G.Q. *Research on the Theory and Methods of Layout Design and Their Applications*; Dalian University of Technology: Dalian, China, 2003. (In Chinese)
58. Zanjirani Farahani, R.; Hekmatfar, M. *Facilities Location: Concepts, Models and Applications*; Springer: Berlin/Heidelberg, Germany, 2009.
59. Hengeveld, D.W.; Braun, J.E.; Groll, E.A.; Williams, A.D. Optimal Placement of Electronic Components to Minimize heat flux nonuniformities. *J. Spacecr. Rocket.* **2011**, *48*, 556–563. [[CrossRef](#)]
60. Hengeveld, D.W.; Braun, J.E.; Groll, E.A.; Williams, A.D. Optimal Distribution of Electronic Components to Balance Environmental Fluxes. *J. Spacecr. Rocket.* **2011**, *48*, 694–697. [[CrossRef](#)]

**Disclaimer/Publisher's Note:** The statements, opinions and data contained in all publications are solely those of the individual author(s) and contributor(s) and not of MDPI and/or the editor(s). MDPI and/or the editor(s) disclaim responsibility for any injury to people or property resulting from any ideas, methods, instructions or products referred to in the content.